Supplement of Geosci. Model Dev., 18, 6737–6765, 2025
https://doi.org/10.5194/gmd-18-6737-2025-supplement

Geoscientific Model Development
Open Access
EGU

Supplement of

Evaluation of ozone and its precursors using the Multi-Scale Infrastructure for Chemistry and Aerosols Version 0 (MUSICAv0) during the Michigan–Ontario Ozone Source Experiment (MOOSE)

Noribeth Mariscal et al.

Correspondence to: Yaoxian Huang (yaoxian.huang@wayne.edu)

Contents in this File:

- Tables S1-S8
- Figures S1-S31

Table S1: Total anthropogenic nitric oxide (NO) emissions from the CAMSv5.1 in Michigan and Southeast Michigan, and their ratio from various sectors*.

	MICH [kt]	SEMI [kt]	SEMI/MICH
AGS	0.46	0.04	9.0%
AWB[1]	0.10	0.01	10.8%
ENE	9.44	2.86	30.3%
RES	1.03	0.48	47.1%
TNR	1.99	0.36	18.1%
TRO	15.13	3.50	23.2%

*AGS = Agriculture Soils; AWB = Agriculture Waste Burning; ENE = Power Generation; RES = Residential; TNR = Off-Road Transportation; TRO = Road Transportation

[1]It is possible that AWB emissions could be double counted via biomass burning emissions from QFED (QuickFire Emissions Dataset), where the fire radiative power obtained from the satellite is used to estimate the global gridded fire emissions (Darmenov and da Silva, 2015). Although it has been found that AWB can increase fire emissions over regions, in Southeast Michigan this contribution is minimal.

Table S2: Mean biases (MB), root-mean squared errors (RMSE), and Pearson correlations (CORR) for surface O_3 concentrations compared to observations from available MI EGLE stationary sites (Model – Observations).

		MB	RMSE	CORR
Allen Park	**ne30x8**	-3.66	13.09	0.73
	ne30x8 DIUR	-2.32	12.10	0.73
	ne30x16	-6.38	13.64	0.72
	ne30x16 DIUR	-5.57	12.91	0.71
Detroit–E 7 Mile	**ne30x8**	0.17	13.17	0.72
	ne30x8 DIUR	1.74	12.54	0.72
	ne30x16	-2.60	13.17	0.71
	ne30x16 DIUR	-1.58	12.15	0.72
New Haven	**ne30x8**	0.89	11.28	0.77
	ne30x8 DIUR	2.38	11.67	0.76
	ne30x16	-0.85	11.56	0.75
	ne30x16 DIUR	-0.22	11.40	0.74
Oak Park	**ne30x8**	0.26	12.69	0.74
	ne30x8 DIUR	1.97	11.99	0.75
	ne30x16	-1.12	11.56	0.76
	ne30x16 DIUR	0.02	11.10	0.75
Port Huron	**ne30x8**	-3.12	12.57	0.72
	ne30x8 DIUR	-2.14	12.15	0.71
	ne30x16	-6.26	13.97	0.69
	ne30x16 DIUR	-5.57	13.63	0.67
Warren	**ne30x8**	2.55	12.67	0.74
	ne30x8 DIUR	4.09	12.32	0.75
	ne30x16	-0.52	12.12	0.73
	ne30x16 DIUR	0.47	11.32	0.73
Ypsilanti	**ne30x8**	3.69	10.92	0.77
	ne30x8 DIUR	5.63	11.46	0.78
	ne30x16	2.46	10.91	0.75
	ne30x16 DIUR	3.13	10.97	0.75

Table S3: Same as Table S2, but for NO_2.

		MB	RMSE	CORR
Detroit–E 7 Mile	**ne30x8**	2.48	6.25	0.61
	ne30x8 DIUR	1.93	5.14	0.59
	ne30x16	2.65	6.96	0.57
	ne30x16 DIUR	1.87	5.75	0.53
Detroit - SW	**ne30x8**	2.56	6.89	0.54
	ne30x8 DIUR	1.81	5.82	0.47
	ne30x16	3.85	8.12	0.56
	ne30x16 DIUR	2.94	7.13	0.48
DP4th	**ne30x8**	1.52	7.31	0.54
	ne30x8 DIUR	0.29	6.39	0.45
	ne30x16	3.67	8.31	0.54
	ne30x16 DIUR	2.67	7.40	0.46
Eliza Howell–NR	**ne30x8**	-10.32	12.81	0.05
	ne30x8 DIUR	-10.85	13.11	0.05
	ne30x16	-10.35	12.73	0.06
	ne30x16 DIUR	-10.83	13.03	0.06
Military Park	**ne30x8**	1.98	7.02	0.60
	ne30x8 DIUR	0.65	5.63	0.56
	ne30x16	4.13	8.31	0.57
	ne30x16 DIUR	3.03	6.95	0.54
Trinity St. Marks	**ne30x8**	1.98	7.31	0.41
	ne30x8 DIUR	1.38	6.01	0.41
	ne30x16	2.83	8.07	0.46
	ne30x16 DIUR	2.23	6.88	0.47

Table S4: Pearson correlations (CORR), standard deviations (STD), normalized standard deviations (CV), root-mean squared errors (RMSE) and normalized root-mean squared errors (NRMSE) of the model simulations compared to available gas-phase chemical species from the Aerodyne Mobile Laboratory (AML).

		CORR	STD	CV	RMSE	NRMSE
O_3	**ne30x8**	0.74	19.12	55.04	12.83	0.84
	ne30x8 DIUR	0.76	17.56	48.23	11.72	0.77
	ne30x16	0.74	17.86	56.65	12.91	0.85
	ne30x16 DIUR	0.73	15.98	48.82	11.84	0.78
HCHO	**ne30x8**	0.58	1.46	57.37	1.26	1.02
	ne30x8 DIUR	0.59	1.48	58.49	1.27	1.02
	ne30x16	0.61	0.91	45.55	1.07	0.86
	ne30x16 DIUR	0.58	0.91	44.93	1.1	0.89
NO	**ne30x8**	0.29	4.51	161.75	10.5	1.03
	ne30x8 DIUR	0.35	4	159.77	10.31	1.01
	ne30x16	0.3	6.13	169.44	10.55	1.04
	ne30x16 DIUR	0.32	5.03	168.98	10.36	1.02
NO_2	**ne30x8**	0.46	7.99	63.76	8.07	1.1
	ne30x8 DIUR	0.49	5.71	50.37	6.73	0.92
	ne30x16	0.58	9.49	68.33	8.36	1.14
	ne30x16 DIUR	0.59	7.12	58.69	6.59	0.9
NO_x	**ne30x8**	0.23	9.92	65.13	14.49	1.12
	ne30x8 DIUR	0.26	7.59	54.55	13.53	1.05
	ne30x16	0.32	12.58	73.43	14.93	1.15
	ne30x16 DIUR	0.31	9.63	63.8	13.66	1.06
C_2H_6	**ne30x8**	0.36	0.39	44.06	9.49	1.38
	ne30x8 DIUR	0.36	0.38	43.04	9.5	1.38
	ne30x16	0.36	0.37	44.62	9.53	1.39
	ne30x16 DIUR	0.38	0.36	43.63	9.53	1.39
C_3H_8	**ne30x8**	0.27	0.33	67.38	1.65	1.3
	ne30x8 DIUR	0.28	0.33	67.79	1.65	1.3
	ne30x16	0.28	0.46	76.68	1.58	1.25
	ne30x16 DIUR	0.32	0.43	72.08	1.56	1.23
C_3H_6	**ne30x8**	0.19	0.17	68.82	0.36	1.06
	ne30x8 DIUR	0.21	0.18	68.58	0.35	1.05
	ne30x16	0.19	0.21	77.27	0.36	1.08
	ne30x16 DIUR	0.21	0.2	75.87	0.36	1.07

BENZ	**ne30x8**	0.21	0.12	58.16	0.17	1.65
	ne30x8 DIUR	0.21	0.12	57.53	0.17	1.64
	ne30x16	0.2	0.15	67.87	0.2	1.94
	ne30x16 DIUR	0.23	0.15	66.83	0.2	1.93
TOLU	**ne30x8**	0.03	0.51	77.81	0.92	1.46
	ne30x8 DIUR	0.03	0.5	77.59	0.91	1.45
	ne30x16	0.02	0.73	87.91	1.14	1.82
	ne30x16 DIUR	0.03	0.69	82.95	1.11	1.77
ISOP	**ne30x8**	0.25	0.39	157.91	0.41	4.06
	ne30x8 DIUR	0.29	0.34	148.24	0.35	3.48
	ne30x16	0.4	0.12	133.75	0.12	1.2
	ne30x16 DIUR	0.38	0.12	131.84	0.12	1.23
APIN	**ne30x8**	0.28	0.03	77.87	0.04	2.33
	ne30x8 DIUR	0.33	0.02	69.02	0.03	1.97
	ne30x16	0.25	0.05	85.88	0.06	3.65
	ne30x16 DIUR	0.32	0.04	76.05	0.06	3.17

Table S5: Same as Table S4, but for available meteorological parameters.

		CORR	STD	CV	RMSE	NRMSE
RH	**ne30x8**	0.76	17.99	30.17	13.63	0.73
	ne30x8 DIUR	0.76	18.04	30.17	13.58	0.73
	ne30x16	0.78	17.73	29.92	13.27	0.71
	ne30x16 DIUR	0.78	17.77	29.95	13.2	0.71
H_2O	**ne30x8**	0.89	6501335.69	39.68	3602571.29	0.72
	ne30x8 DIUR	0.89	6430226.01	39.25	3544576.07	0.71
	ne30x16	0.89	6327619.47	38.9	3371758	0.68
	ne30x16 DIUR	0.9	6349449.03	39.1	3355553.72	0.67
WS	**ne30x8**	0.44	3.04	52.27	4.53	3.87
	ne30x8 DIUR	0.44	2.99	51.07	4.53	3.87
	ne30x16	0.43	2.79	49.56	4.24	3.62
	ne30x16 DIUR	0.43	2.8	49.91	4.23	3.61
WD	**ne30x8**	0.55	94.09	49.46	78.73	1.46
	ne30x8 DIUR	0.57	93.56	49.64	77.2	1.43
	ne30x16	0.55	92.78	48.91	77.74	1.44
	ne30x16 DIUR	0.55	93.3	49.92	77.96	1.44
PS	**ne30x8**	0.97	650.84	0.66	234.82	0.4
	ne30x8 DIUR	0.97	651.4	0.66	234.29	0.4
	ne30x16	0.97	652.36	0.66	300.53	0.51
	ne30x16 DIUR	0.97	656.02	0.66	299.16	0.51
T	**ne30x8**	0.92	5.07	1.72	2.35	0.42
	ne30x8 DIUR	0.92	5.08	1.72	2.34	0.41
	ne30x16	0.93	5.11	1.73	2.23	0.39
	ne30x16 DIUR	0.93	5.08	1.72	2.25	0.4

Table S6: Detailed statistics for tropospheric NO_2 and HCHO columns from Pandora and four model simulations at the SWDetroitMI site in Southeast Michigan.

		n	CORR	MB	NMB	RMSE	NRMSE
NO2	**ne30x8**	83	0.27	-7.80E+14	-0.10	4.73E+15	1.18
	ne30x8 DIUR		0.25	-5.69E+14	-0.07	4.58E+15	1.14
	ne30x16		0.28	5.69E+14	0.07	5.07E+15	1.27
	ne30x16 DIUR		0.31	7.31E+14	0.09	4.78E+15	1.19
HCHO	**ne30x8**	43	0.17	-2.30E+15	-0.22	5.90E+15	1.36
	ne30x8 DIUR		0.30	-2.50E+15	-0.23	5.41E+15	1.25
	ne30x16		0.11	-1.20E+15	-0.11	5.98E+15	1.38
	ne30x16 DIUR		0.22	-1.43E+15	-0.13	5.49E+15	1.27

Table S7: Detailed statistics for tropospheric NO_2 and HCHO columns from Pandora and four model simulations at the DearbornMI site in Southeast Michigan.

		n	CORR	MB	NMB	RMSE	NRMSE
NO2	**ne30x8**	160	0.59	-2.89E+13	-0.004	4.16E+15	0.81
	ne30x8 DIUR		0.43	8.10E+14	0.11	4.75E+15	0.92
	ne30x16		0.61	6.50E+14	0.09	4.30E+15	0.83
	ne30x16 DIUR		0.58	1.52E+15	0.21	4.64E+15	0.90
HCHO	**ne30x8**	113	0.19	-3.01E+15	-0.30	4.94E+15	1.52
	ne30x8 DIUR		0.38	-2.18E+15	-0.22	3.98E+15	1.22
	ne30x16		0.15	-2.50E+15	-0.25	5.33E+15	1.64
	ne30x16 DIUR		0.30	-1.74E+15	-0.17	4.65E+15	1.43

Table S8: Detailed information of each GCAS raster on flight days during MOOSE 2021.

		Day of Week	Flight Time	Mean Aircraft Altitude (km)	AQI	Temperature	Wind Direction	Wind Speed
20210605	**Raster 1 (10 EDT)**	Saturday	9:48-11:23 EDT	12.3	108	23-27˚C	SW	6-10 m/s
	Raster 2 (14 EDT)	Saturday	13:47-15:19 EDT	12.3		28-31˚C		6-12 m/s
20210611	**Raster 1 (11 EDT)**	Friday	10:10-11:45 EDT	12.4	71	24-28˚C	NE	2-4 m/s
	Raster 2 (12 EDT)	Friday	11:45-13:16 EDT	12.4		26-29˚C		2-4 m/s
	Raster 3 (13 EDT)	Friday	13:16-14:00 EDT	12.4		27-30˚C		3-5 m/s
20210616	**Raster 1 (10 EDT)**	Wednesday	9:16-11:31 EDT	8.7	51	18-21˚C	N	1-5 m/s
	Raster 2 (13 EDT)	Wednesday	13:05-14:44 EDT	12.1		20-24˚C		3-8 m/s
	Raster 3 (15 EDT)	Wednesday	14:44-16:15 EDT	12.2		20-24˚C		2-8 m/s
20210617	**Raster 1 (10 EDT)**	Thursday	9:18-10:56 EDT	12.3	100	17-21˚C	SW	3-6 m/s

	Raster 2 (11 EDT)	Thursday	10:56-12:29 EDT	12.3		22-25˚C		4-7 m/s
	Raster 3 (15 EDT)	Thursday	14:10-15:44 EDT	12.3		26-28˚C		4-12 m/s
	Raster 1 (9 EDT)	Tuesday	8:51-10:40 EDT	12		11-13˚C		2-7 m/s
20210622	**Raster 2 (11 EDT)**	Tuesday	10:40-12:24 EDT	12	27	15-16˚C	NE	3-7 m/s
	Raster 3 (13 EDT)	Tuesday	12:25-14:44 EDT	11.2		16-17˚C		2-6 m/s
	Raster 1 (9 EDT)	Thursday	8:31-10:23 EDT	10.8		21-23˚C		6-14 m/s
20210624					77		S	
	Raster 2 (11 EDT)	Thursday	10:23-12:24 EDT	9		22-24˚C		8-16 m/s

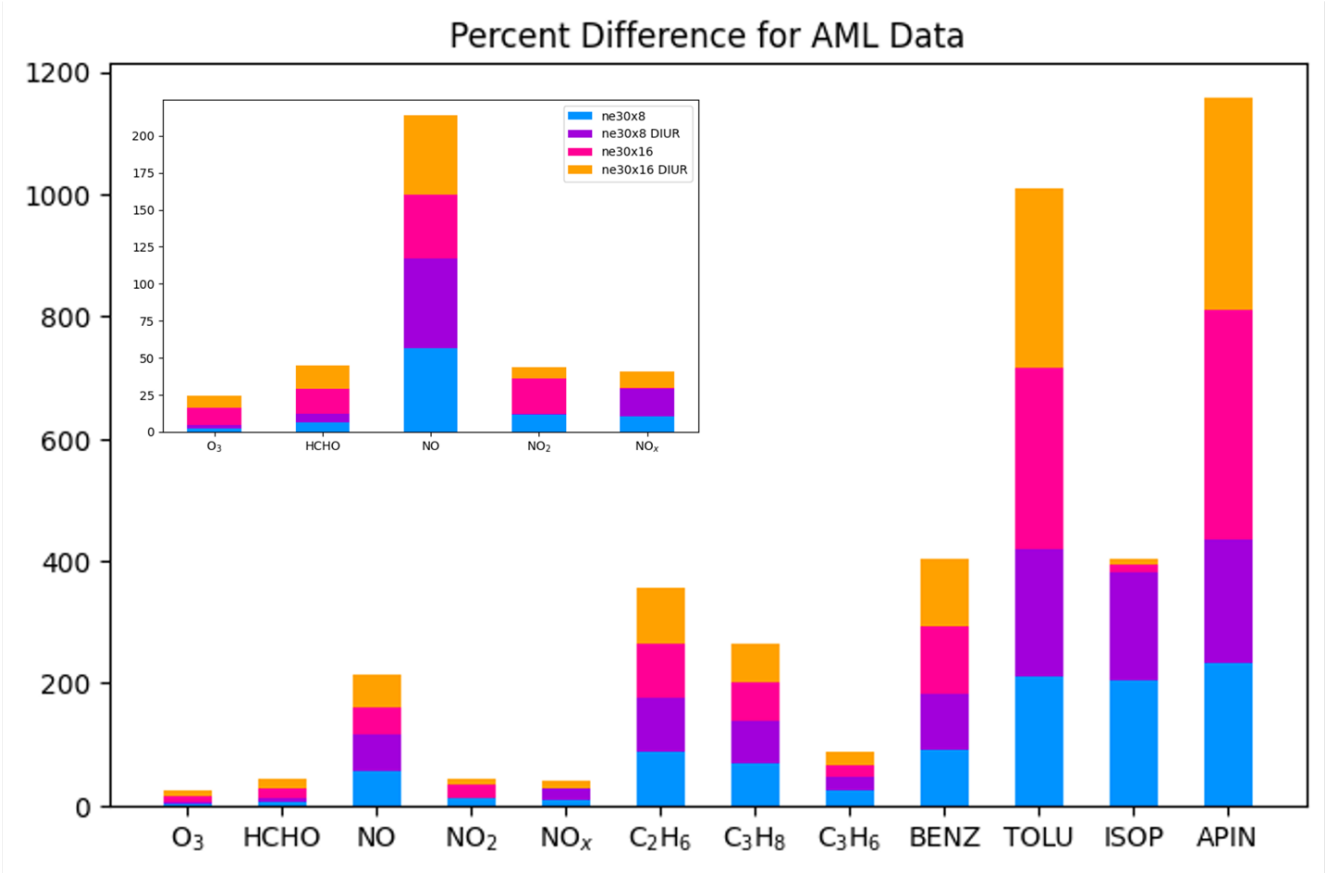

Figure S1: Percent differences between the Aerodyne Mobile Laboratory (AML) observations and MUSICAv0 model simulations used in this study.

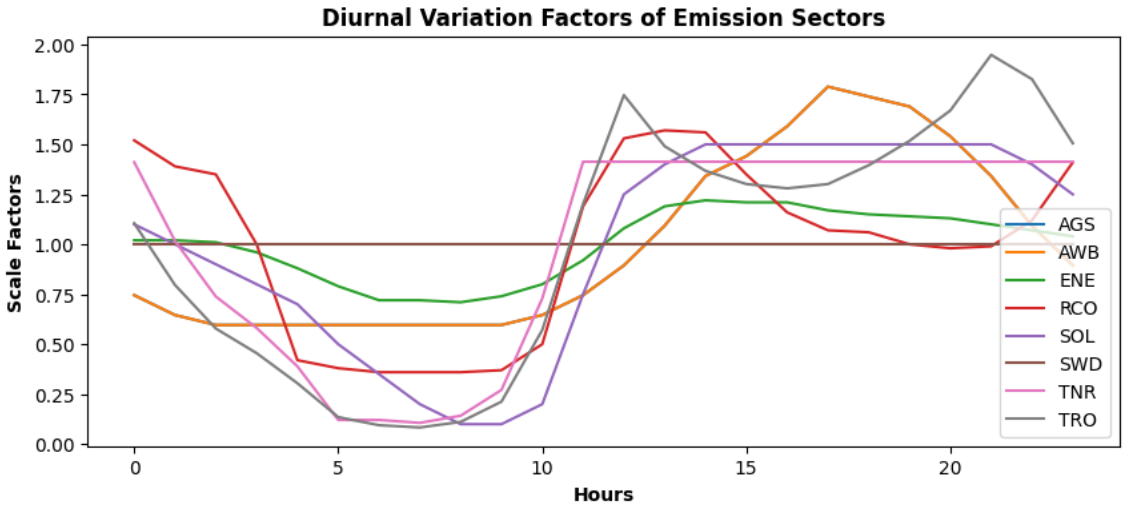

Figure S2: The diurnal variation scale factors applied to NO emissions for each anthropogenic emission sector used in the simulations.

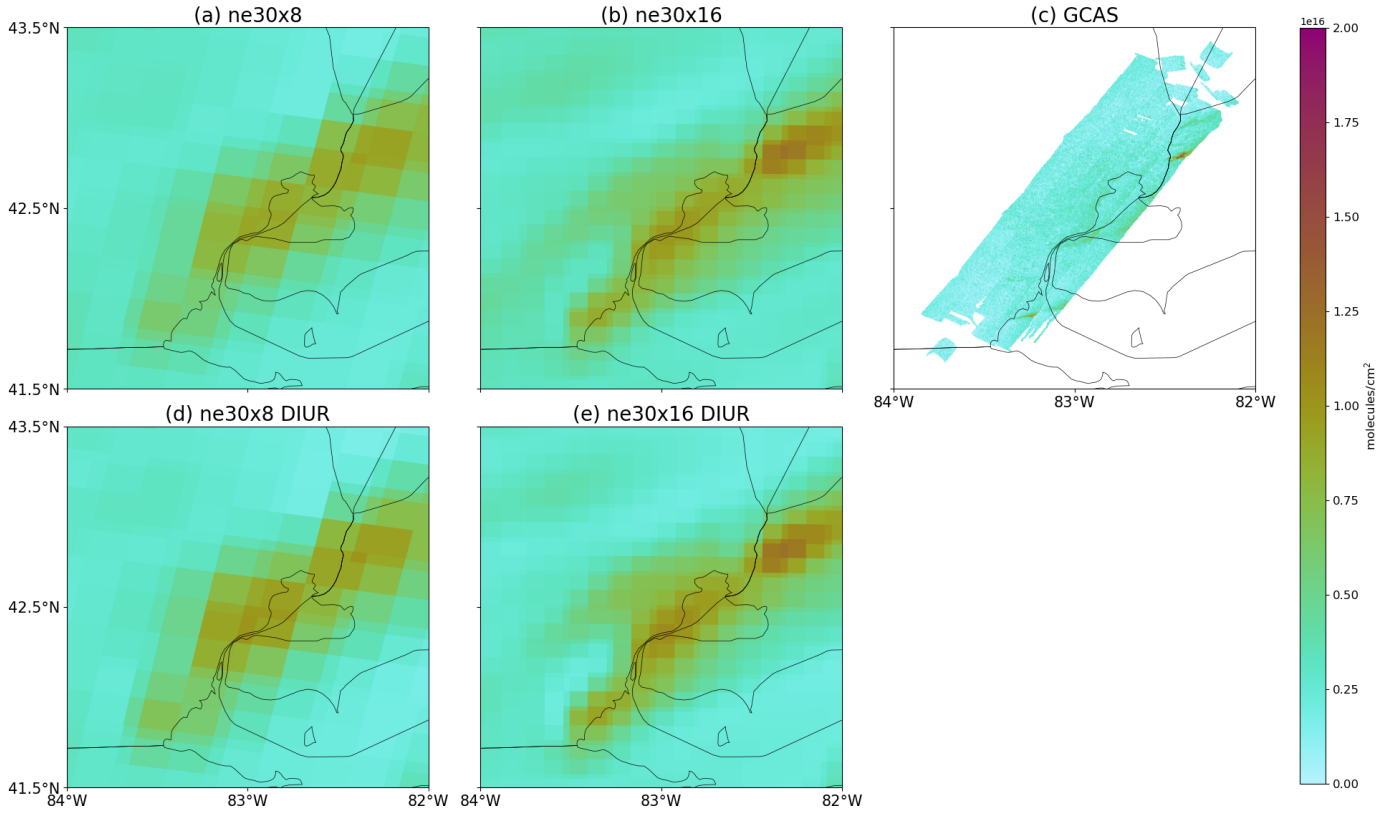

Figure S3: Modeled and observed NO_2 tropospheric columns over Southeast Michigan on 5 June 2021. The GCAS instrument flew over the Southeast Michigan region between 9:48 and 11:23 EDT, so modeled NO_2 tropospheric columns were calculated using the 11 EDT time frame. Panels a, b, d, e represent modeled NO_2 tropospheric columns calculated to about 12 km in altitude, which was the average flight altitude of the NASA Gulfstream-III aircraft. Panel c shows observed NO_2 tropospheric columns from the GCAS instrument during the morning time. Panel f shows the land and lakes.

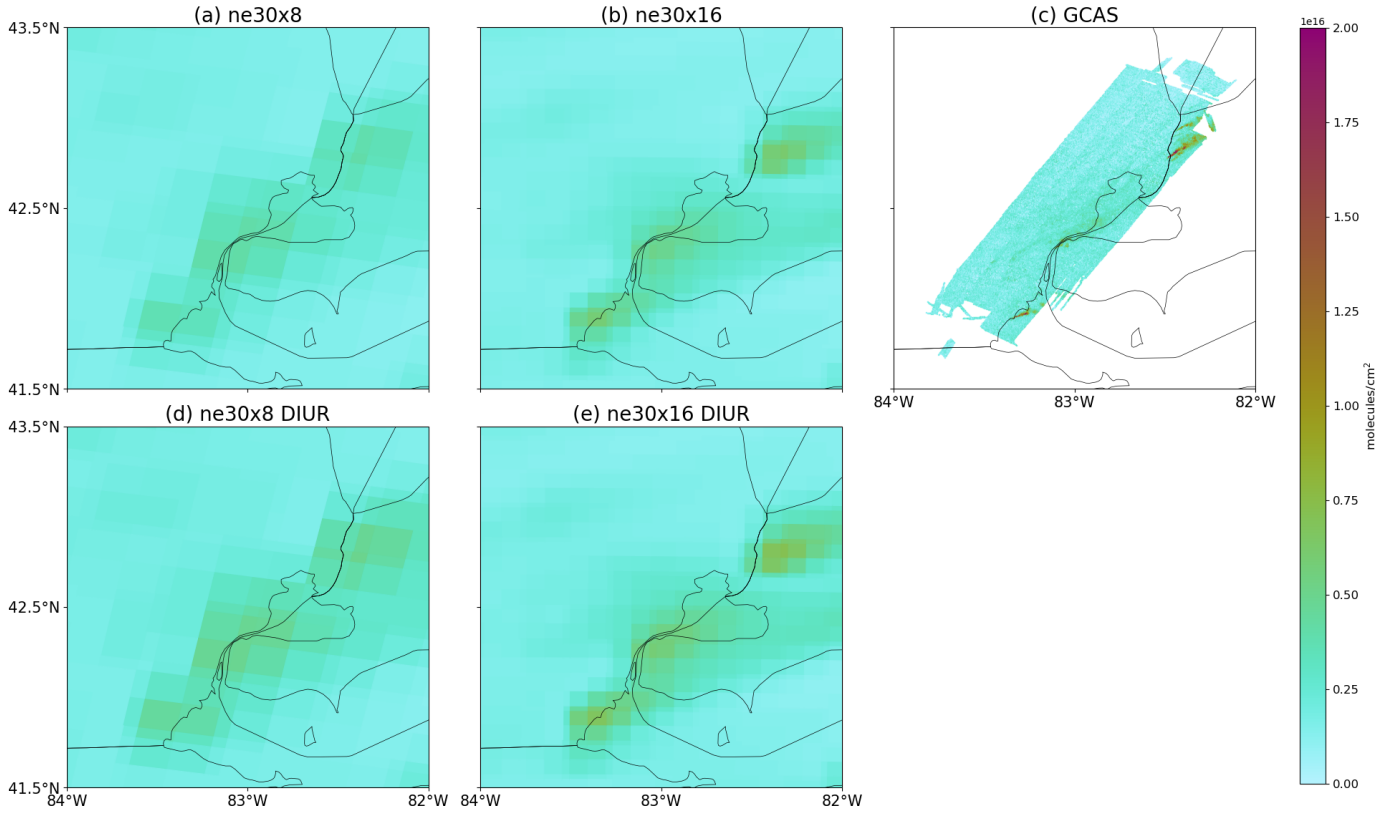

Figure S4: Same as Fig. S3, but the GCAS instrument flew over Southeast Michigan from 13:47 to 15:19 EDT, and modeled NO_2 tropospheric columns were calculated during the 14 EDT time frame.

305
306
307
308
309
310
311
312
313
314
315
316
317
318
319
320
321
322

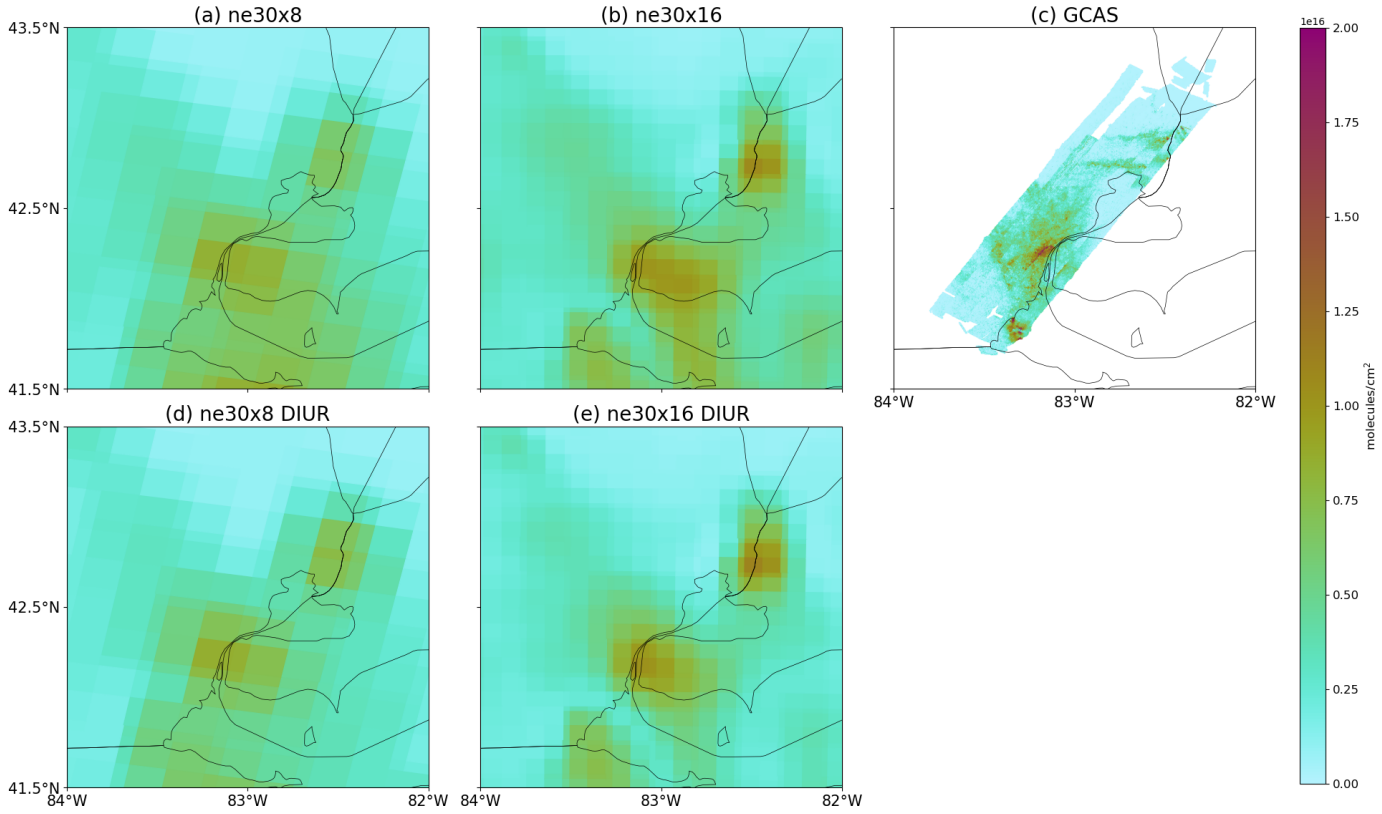

Figure S5: Modeled and observed NO_2 tropospheric columns over Southeast Michigan on 16 June 2021. The GCAS instrument flew over the Southeast Michigan region between 9:16 and 11:31 EDT, so modeled NO_2 tropospheric columns were calculated using the 10 EDT time frame. Figures S4a, S4b, S4d, and S4e represent modeled NO_2 tropospheric columns calculated to about 12 km in altitude, which was the average flight altitude of the NASA Gulfstream-III aircraft. Figure S4c shows observed NO_2 tropospheric columns from the GCAS instrument during the morning time.

340
341
342
343
344
345
346
347
348
349
350
351
352
353
354
355
356
357
358
359

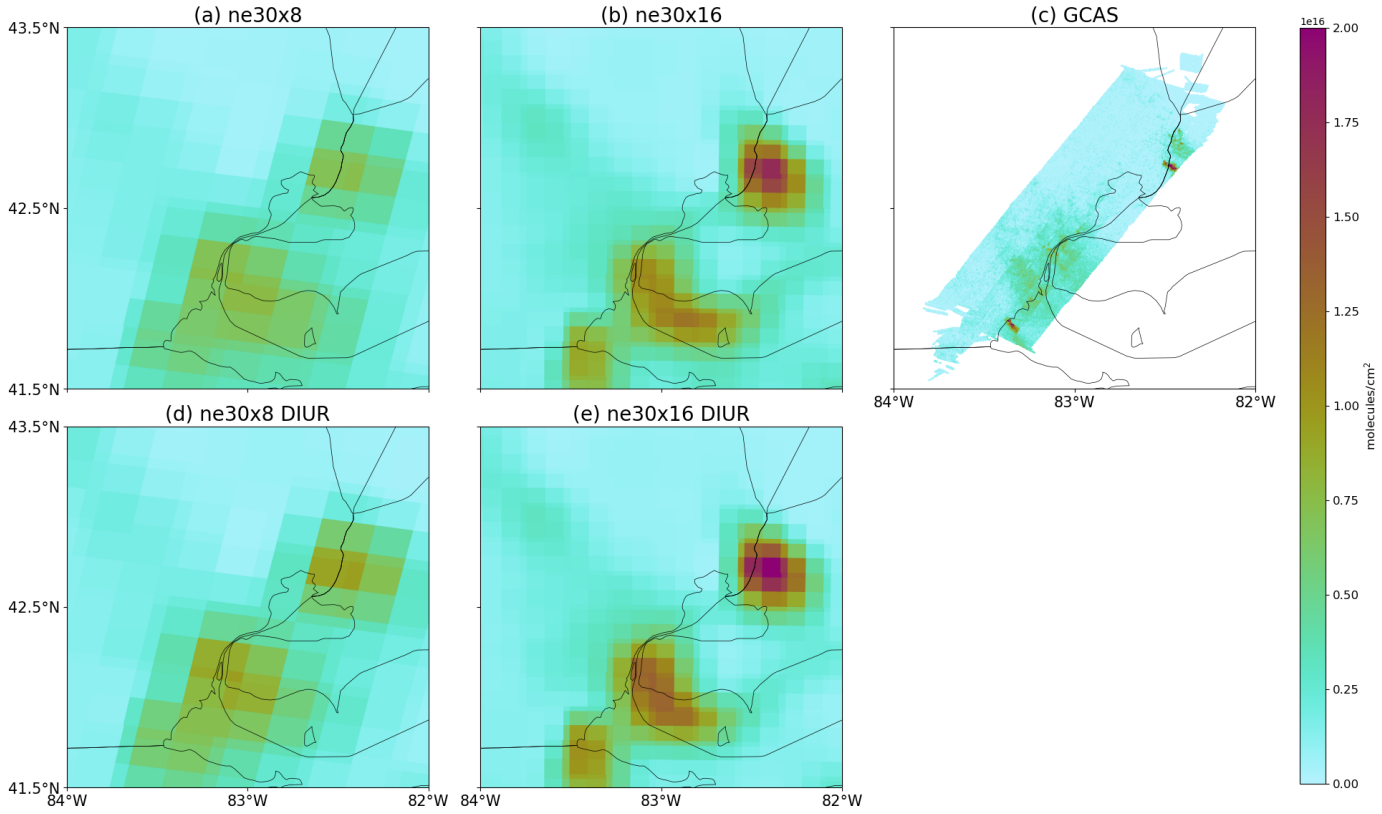

Figure S6: Same as Fig. S5, but the GCAS instrument flew over Southeast Michigan from 13:05 to 14:44 EDT, and modeled NO_2 tropospheric columns were calculated during the 13 EDT time frame.

376
377
378
379
380
381
382
383
384
385
386
387
388
389
390
391
392
393
394

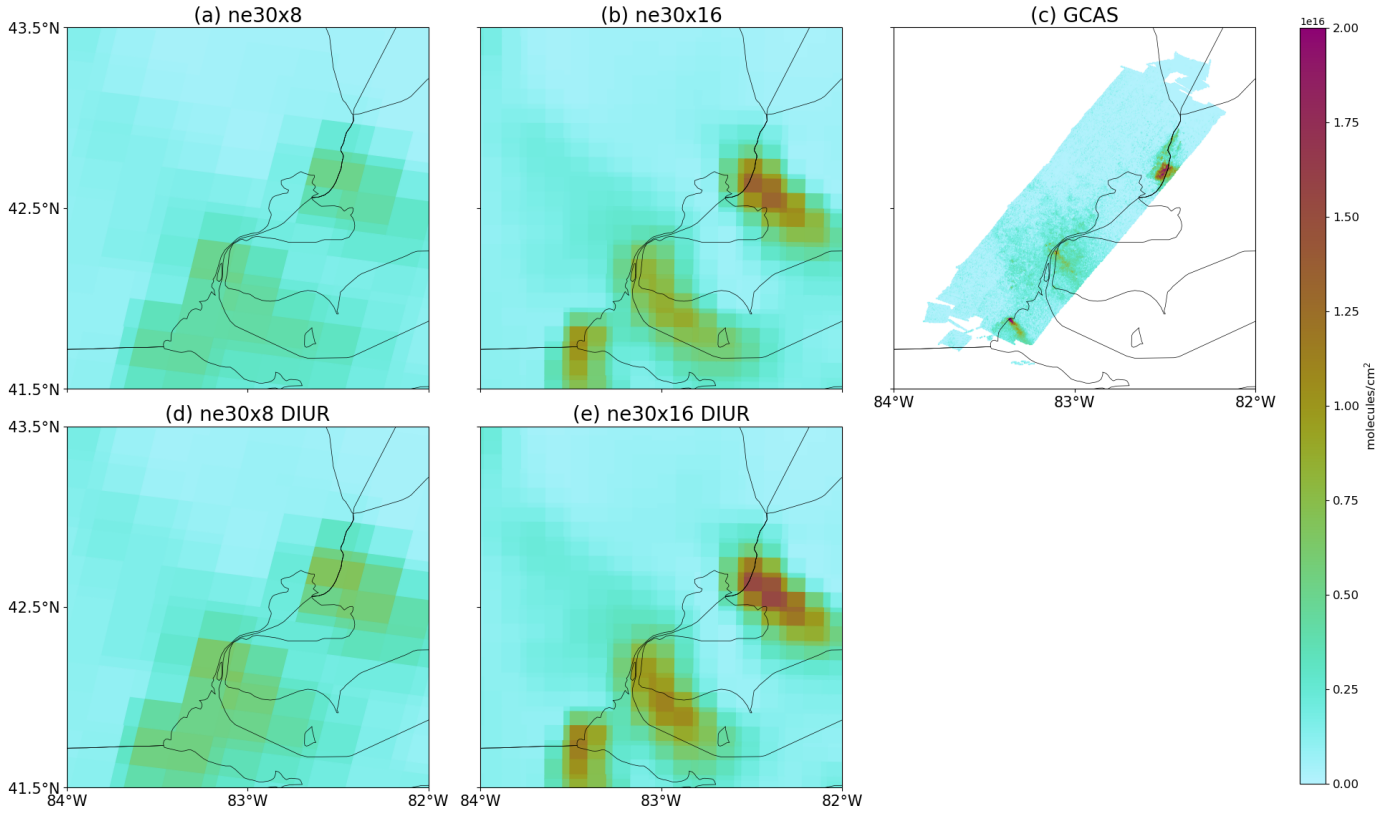

Figure S7: Same as Fig. S5, but the GCAS instrument flew over Southeast Michigan from 14:44 to 16:15 EDT, and modeled NO_2 tropospheric columns were calculated during the 15 EDT time frame.

411
412
413
414
415
416
417
418
419
420
421
422
423
424
425
426
427
428
429

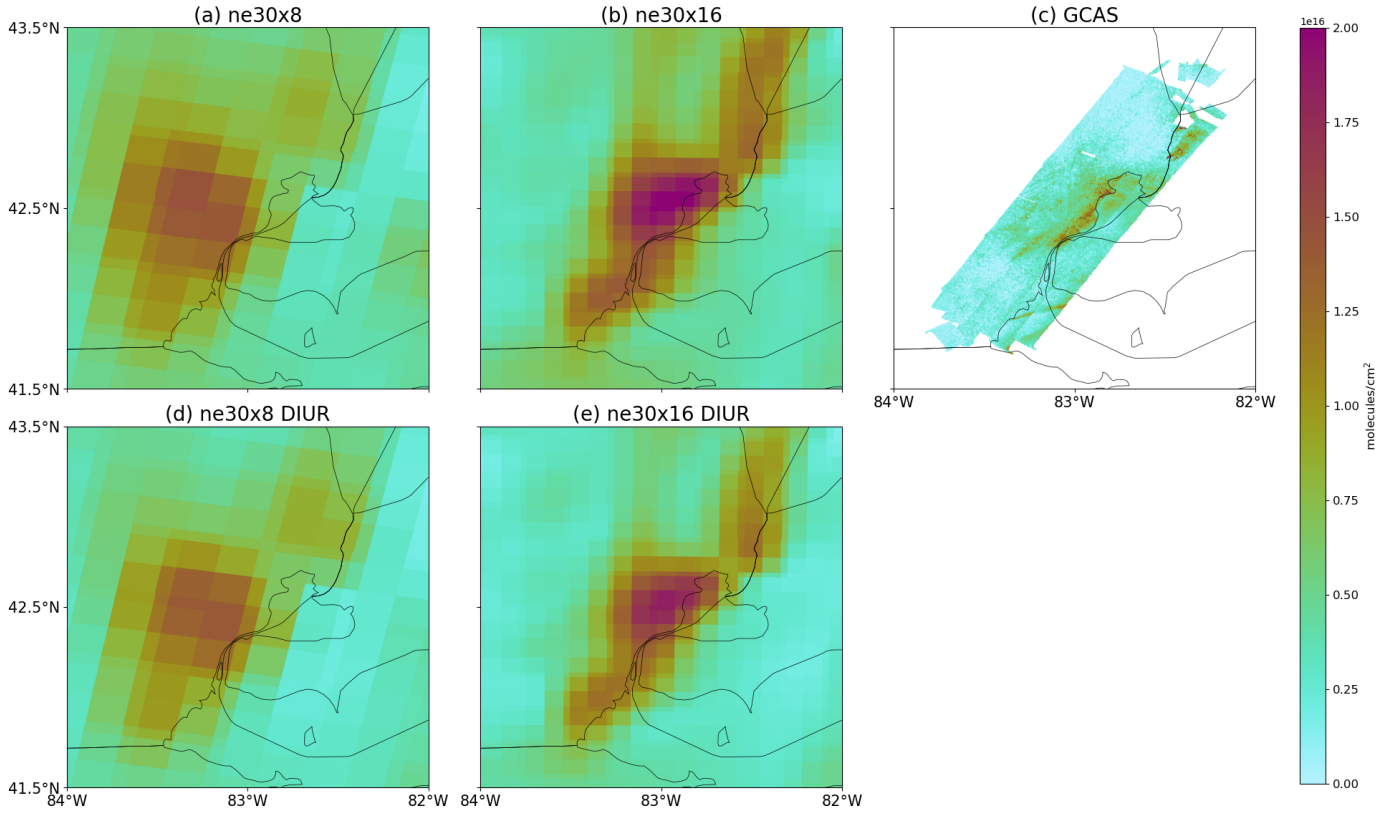

Figure S8: Modeled and observed NO_2 tropospheric columns over Southeast Michigan on 17 June 2021. The GCAS instrument flew over the Southeast Michigan region between 9:18 and 10:56 EDT, so modeled NO_2 tropospheric columns were calculated using the 10 EDT time frame. Figures S7a, S7b, S7d, and S7e represent modeled NO_2 tropospheric columns calculated to about 12 km in altitude, which was the average flight altitude of the NASA Gulfstream-III aircraft. Figure S7c shows observed NO_2 tropospheric columns from the GCAS instrument during the morning time.

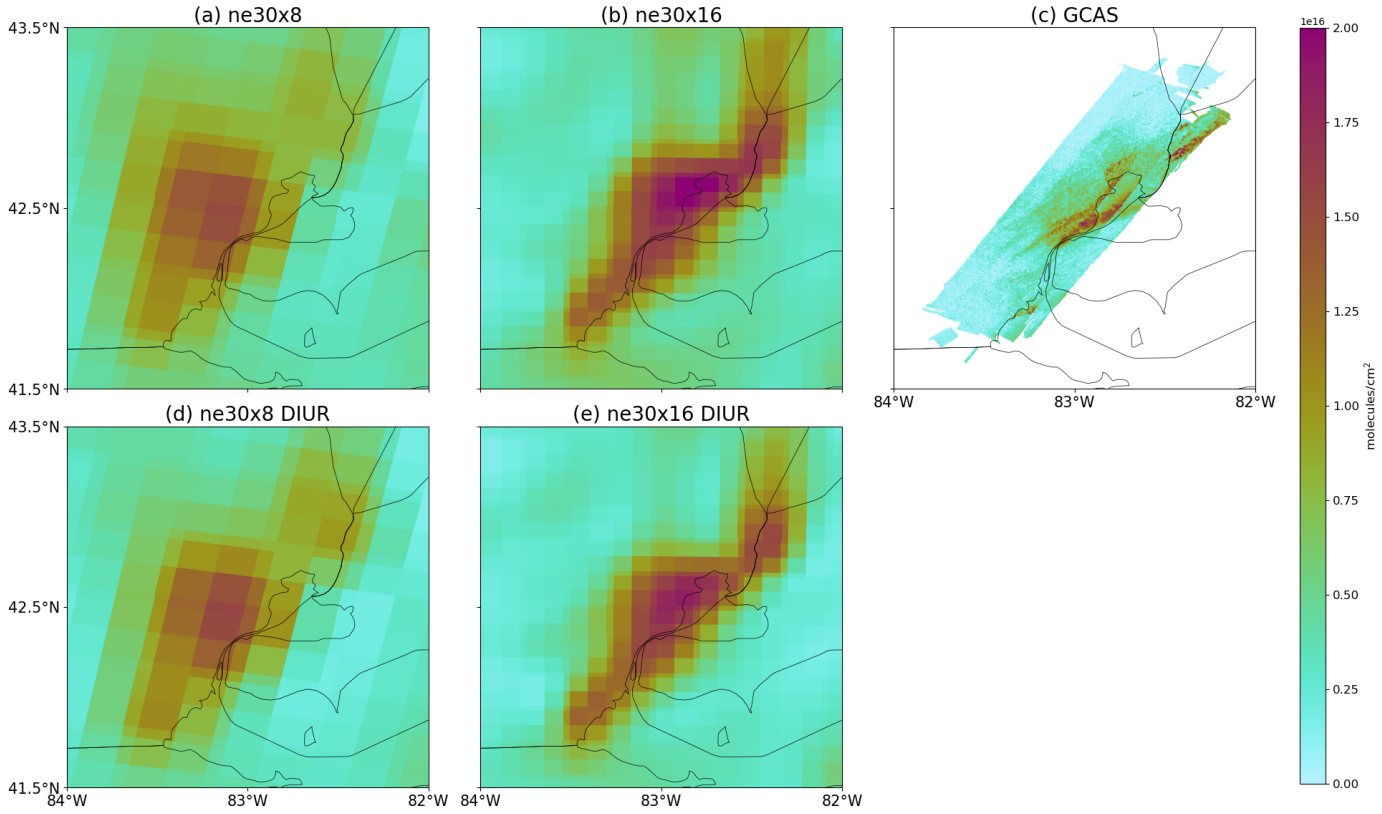

Figure S9: Same as Fig. S7, but the GCAS instrument flew over Southeast Michigan from 10:56 to 12:29 EDT, and modeled NO_2 tropospheric columns were calculated during the 11 EDT time frame.

481
482
483
484
485
486
487
488
489
490
491
492
493
494
495
496
497
498
499

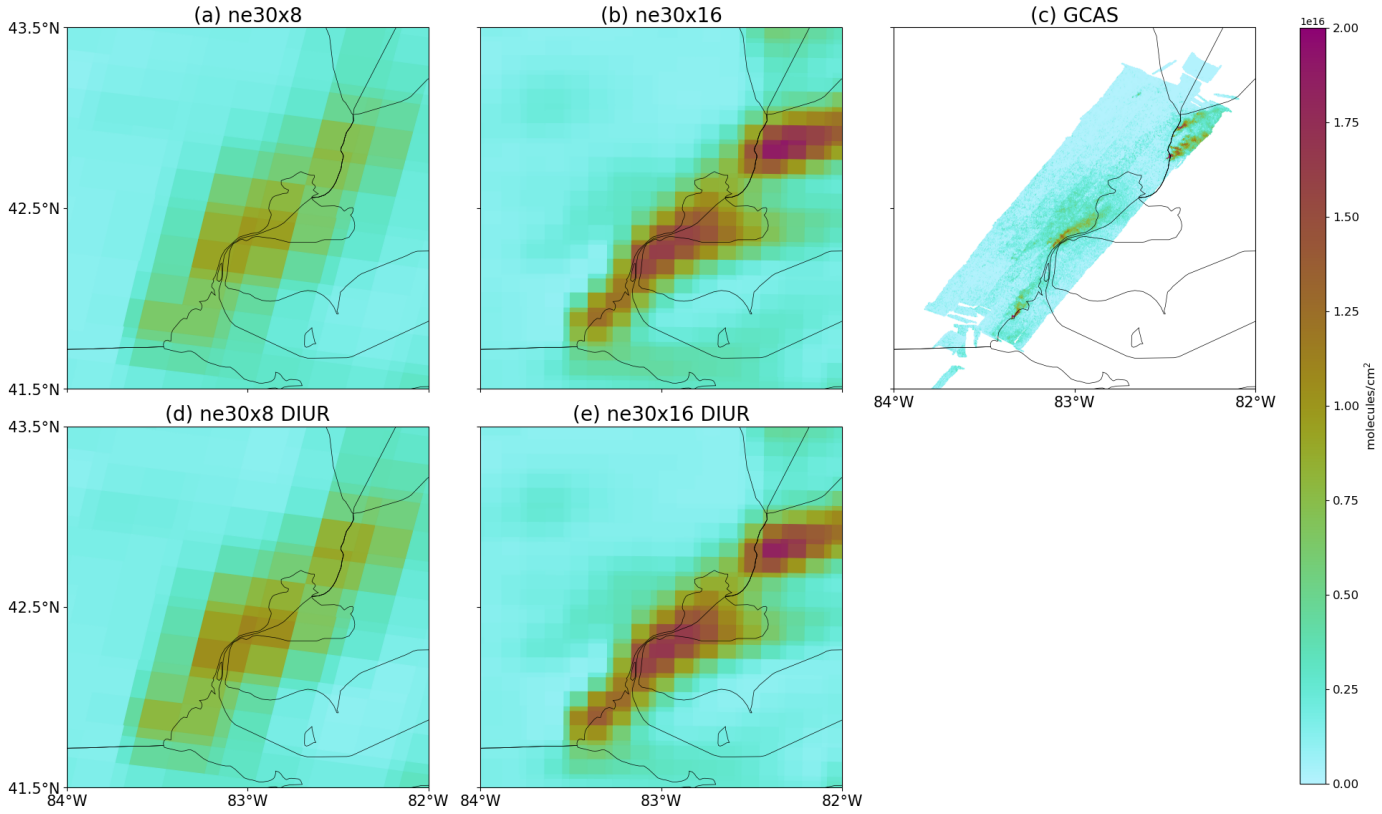

Figure S10: Same as Fig. S7, but the GCAS instrument flew over Southeast Michigan from 14:10 to 15:44 EDT, and modeled NO_2 tropospheric columns were calculated during the 15 EDT time frame.

516
517
518
519
520
521
522
523
524
525
526
527
528
529
530
531
532
533
534

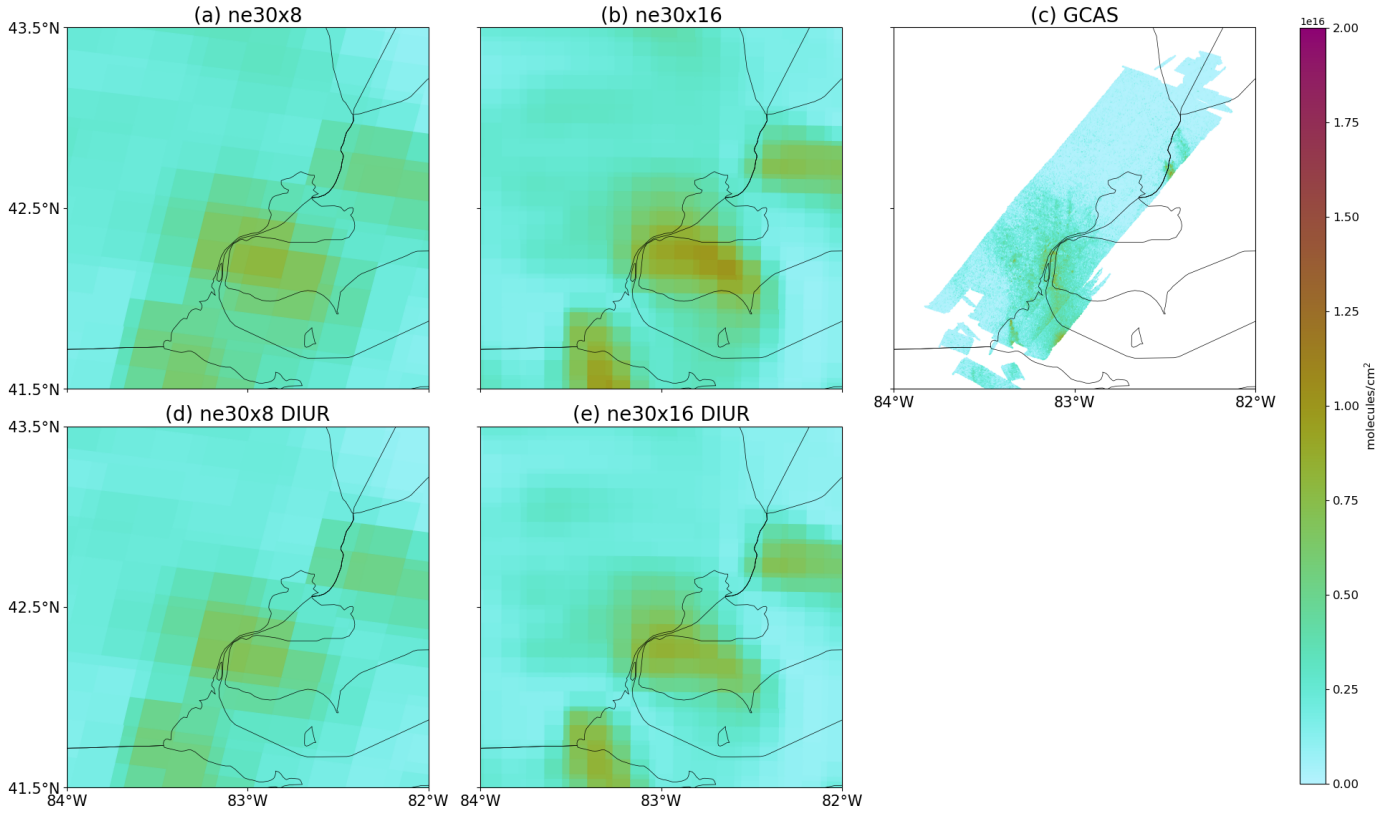

Figure S11: Modeled and observed NO_2 tropospheric columns over Southeast Michigan on 22 June 2021. The GCAS instrument flew over the Southeast Michigan region between 8:51 and 10:41 EDT, so modeled NO_2 tropospheric columns were calculated using the 9 EDT time frame. Figures S10a, S10b, S10d, and S10e represent modeled NO_2 tropospheric columns calculated to about 12 km in altitude, which was the average flight altitude of the NASA Gulfstream-III aircraft. Figure S10c shows observed NO_2 tropospheric columns from the GCAS instrument during the morning time.

552
553
554
555
556
557
558
559
560
561
562
563
564
565
566
567
568
569

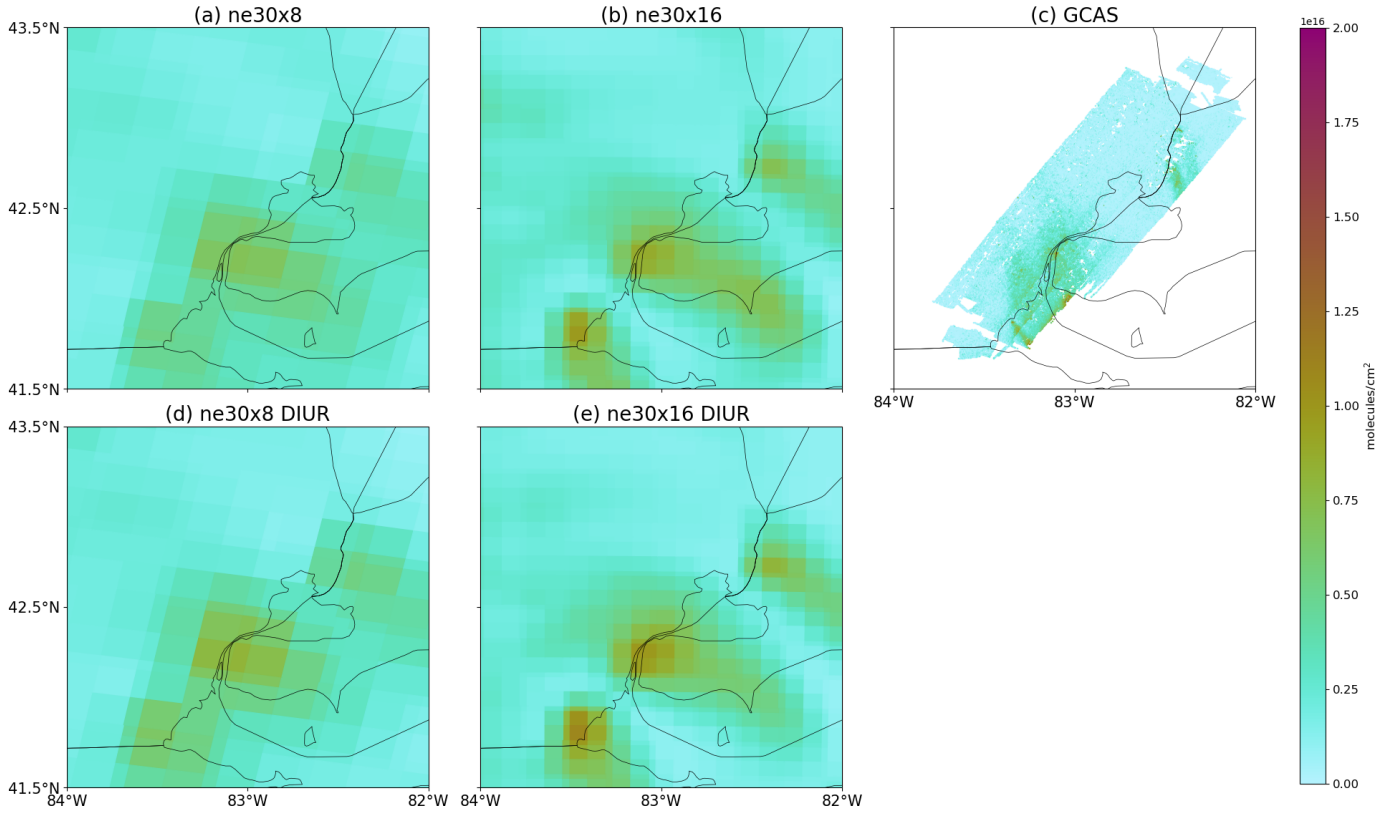

Figure S12: Same as Fig. S10, but the GCAS instrument flew over Southeast Michigan from 10:40 to 12:24 EDT, and modeled NO_2 tropospheric columns were calculated during the 11 EDT time frame.

586
587
588
589
590
591
592
593
594
595
596
597
598
599
600
601
602

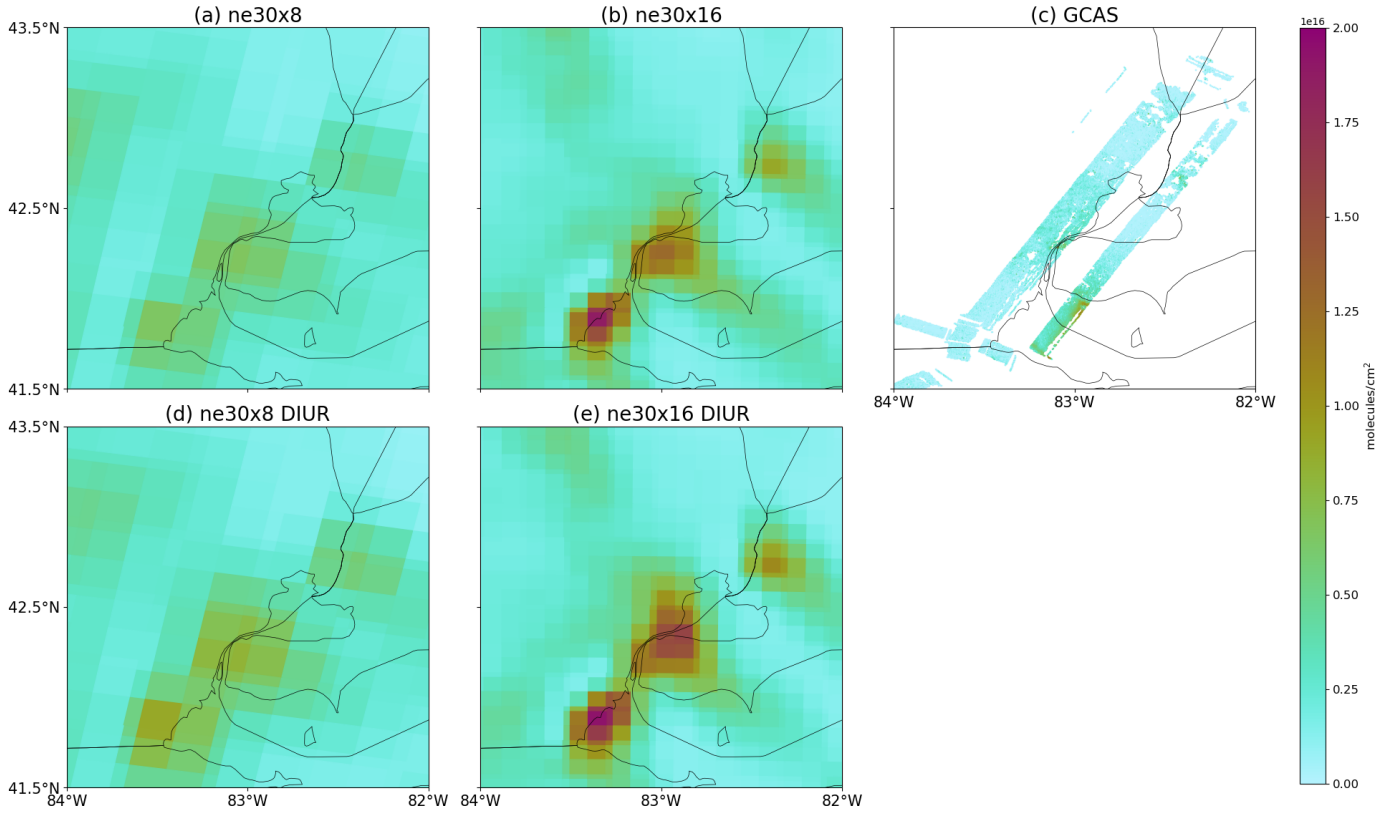

Figure S13: Same as Fig. S10, but the GCAS instrument flew over Southeast Michigan from 12:25 to 14:44 EDT, and modeled NO_2 tropospheric columns were calculated during the 13 EDT time frame.

619
620
621
622
623
624
625
626
627
628
629
630
631
632
633
634
635

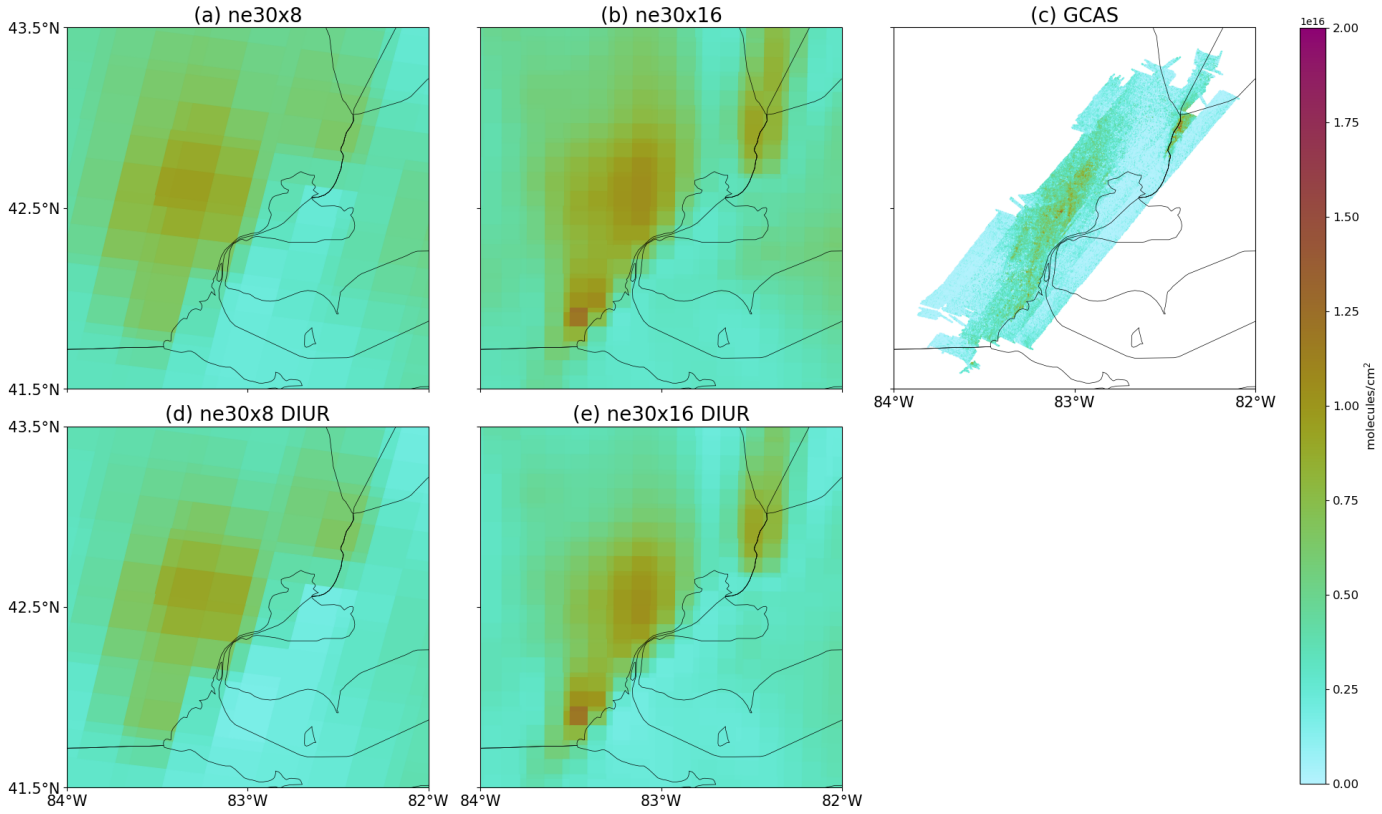

Figure S14: Modeled and observed NO_2 tropospheric columns over Southeast Michigan on 24 June 2021. The GCAS instrument flew over the Southeast Michigan region between 8:31 and 10:23 EDT, so modeled NO_2 tropospheric columns were calculated using the 9 EDT time frame. Figures S13a, S13b, S13d, and S13e represent modeled NO_2 tropospheric columns calculated to about 12 km in altitude, which was the average flight altitude of the NASA Gulfstream-III aircraft. Figure S13c shows observed NO_2 tropospheric column from the GCAS instrument during the morning time.

653
654
655
656
657
658
659
660
661
662
663
664
665
666
667
668
669
670
671

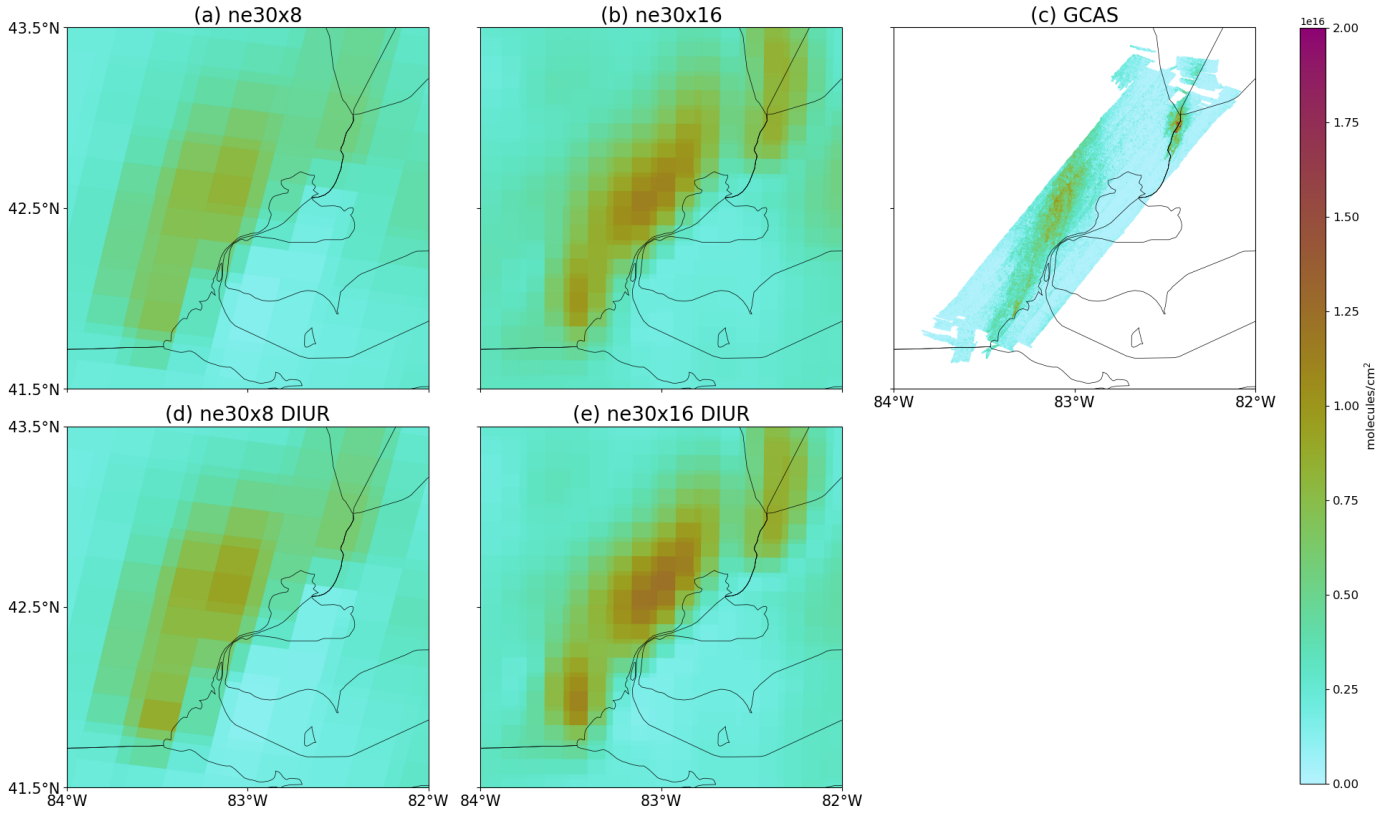

Figure S15: Same as Fig. S13, but the GCAS instrument flew over Southeast Michigan from 10:23 to 12:24 EDT, and modeled NO_2 tropospheric columns were calculated during the 11 EDT time frame.

688
689
690
691
692
693
694
695
696
697
698
699
700
701
702
703
704
705
706

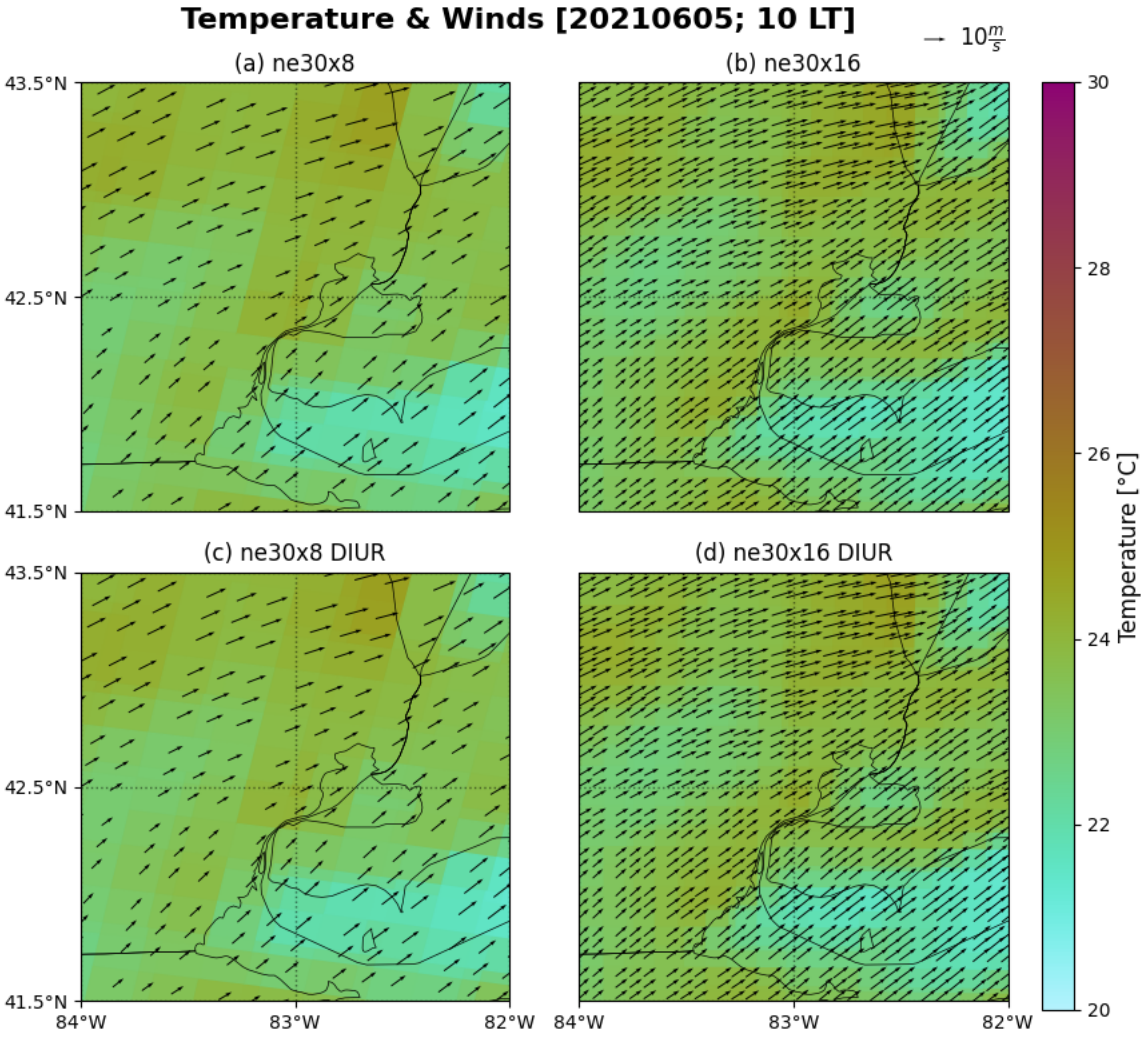

Figure S16: Modeled temperature and wind vectors for 20210605 at 10 LT.

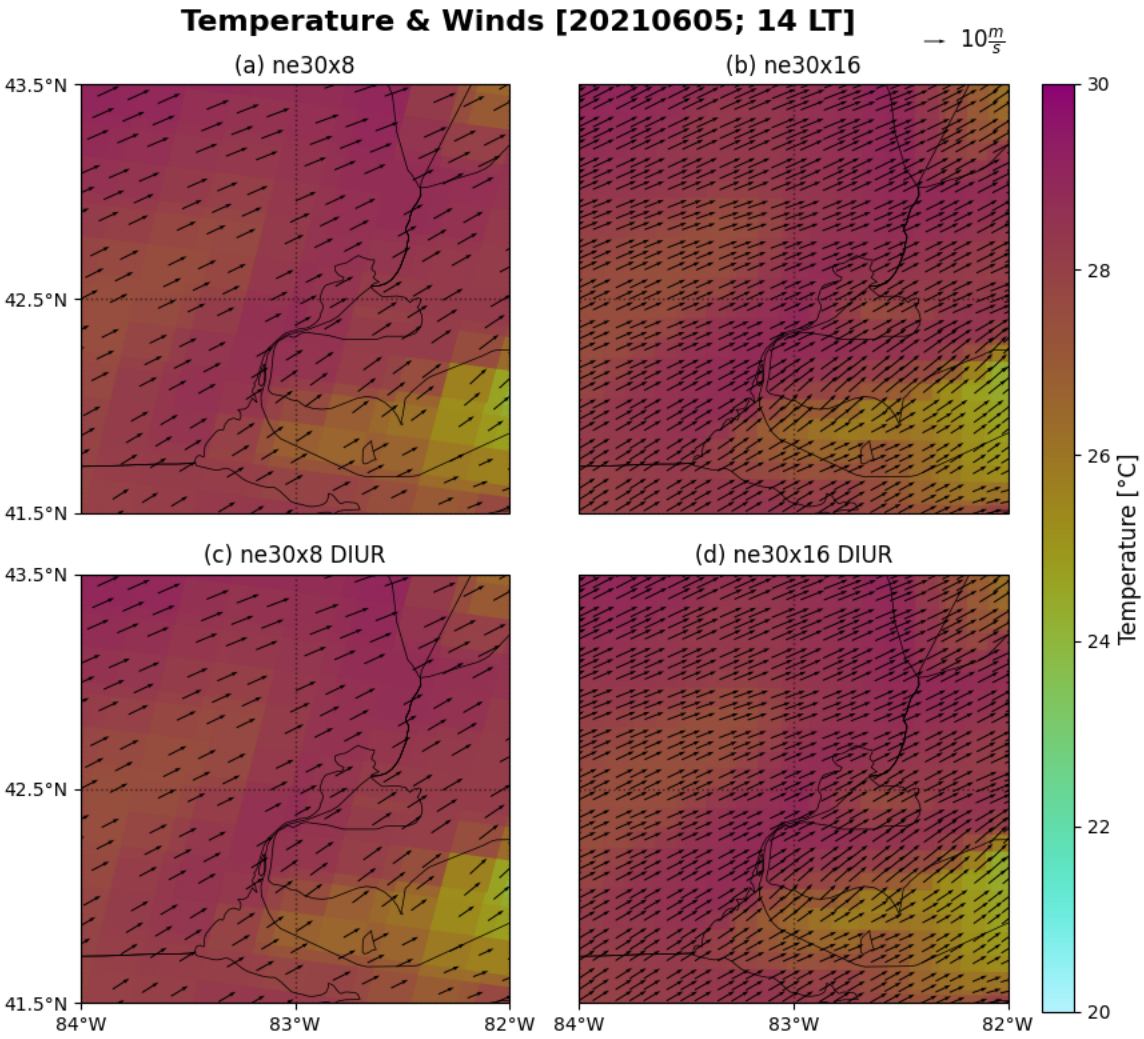

Figure S17: Modeled temperature and wind vectors for 20210605 at 14 LT.

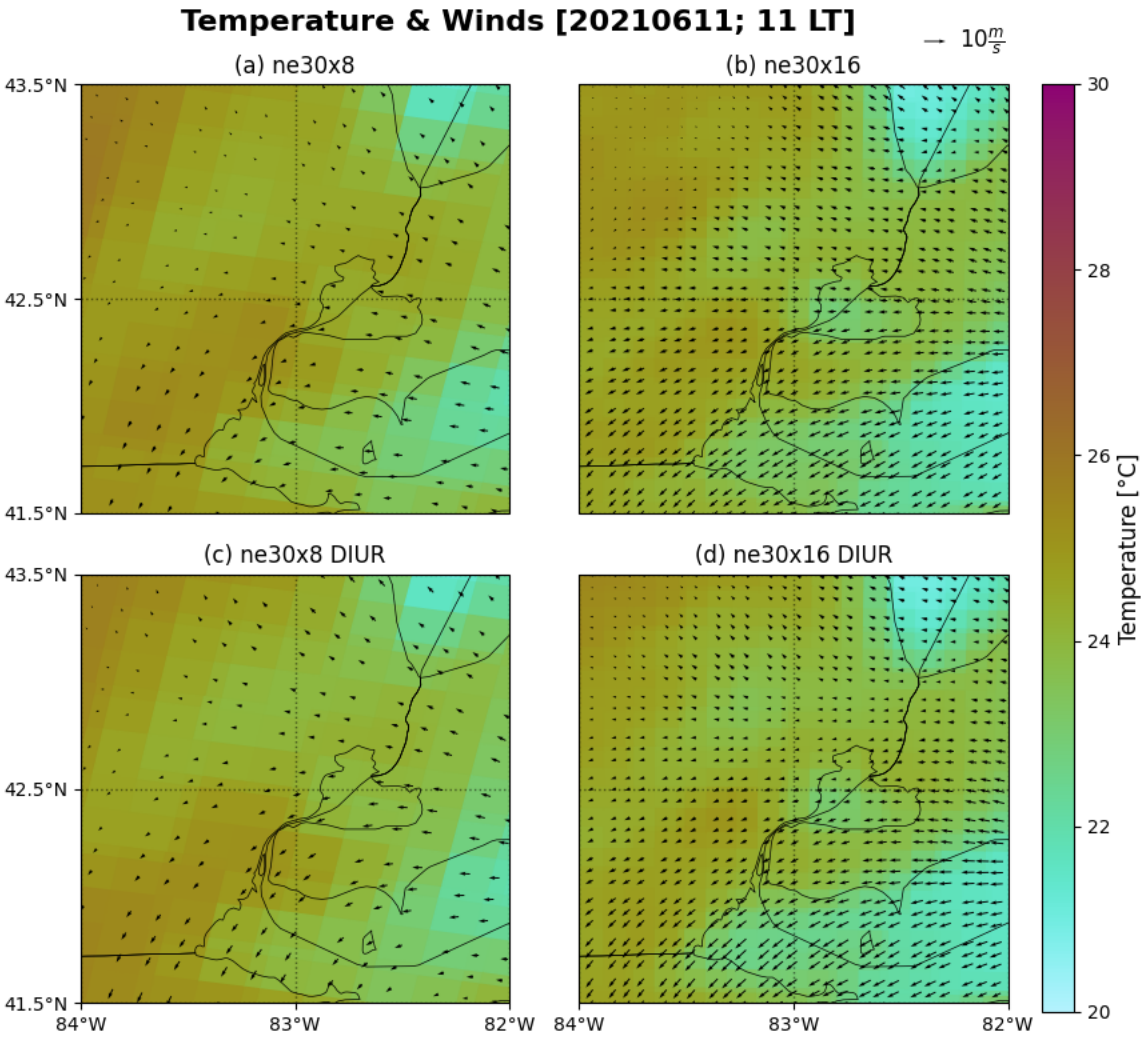

Figure S18: Modeled temperature and wind vectors for 20210611 at 11 LT.

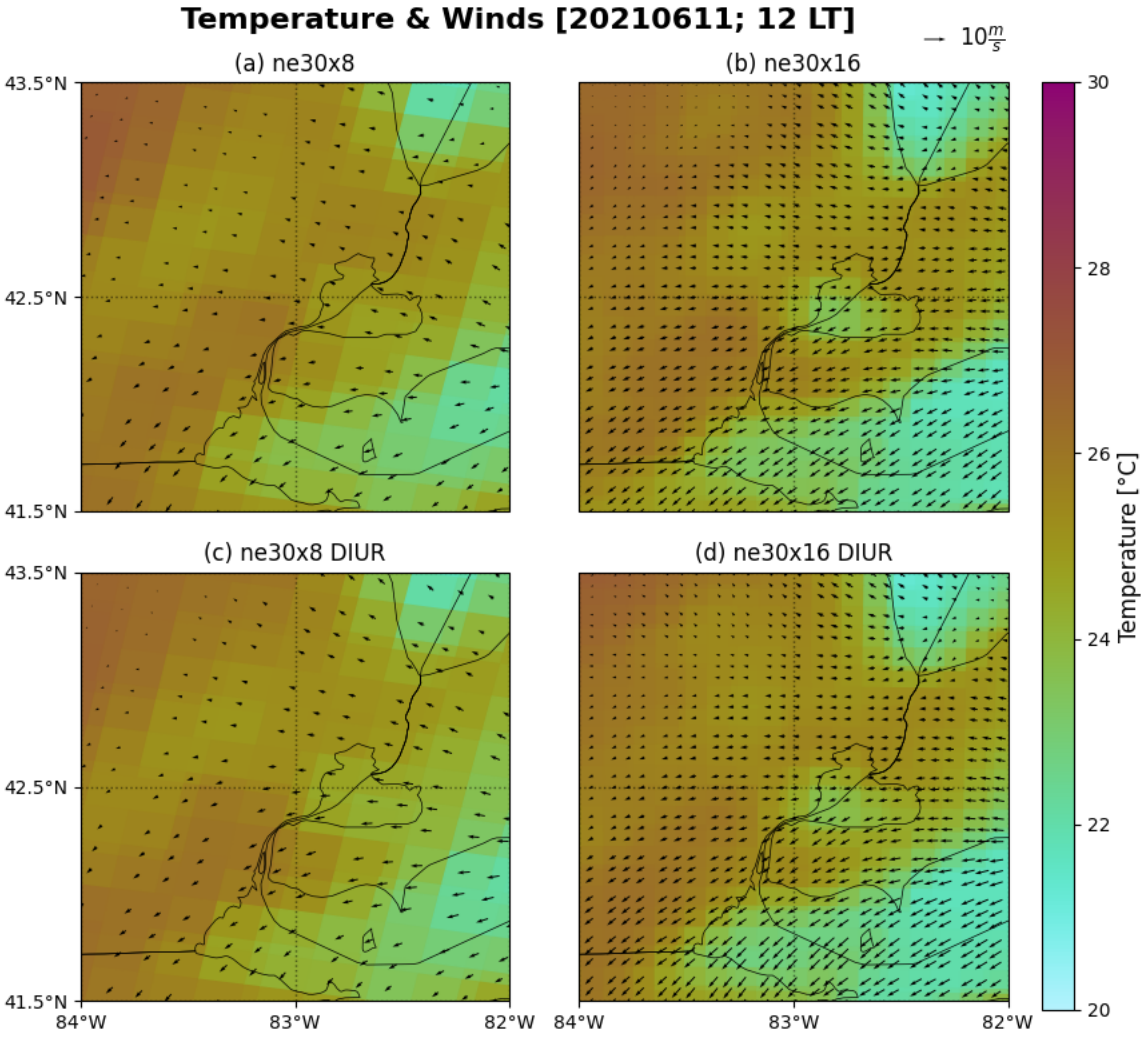

716

717 Figure S19: Modeled temperature and wind vectors for 20210611 at 12 LT.

718

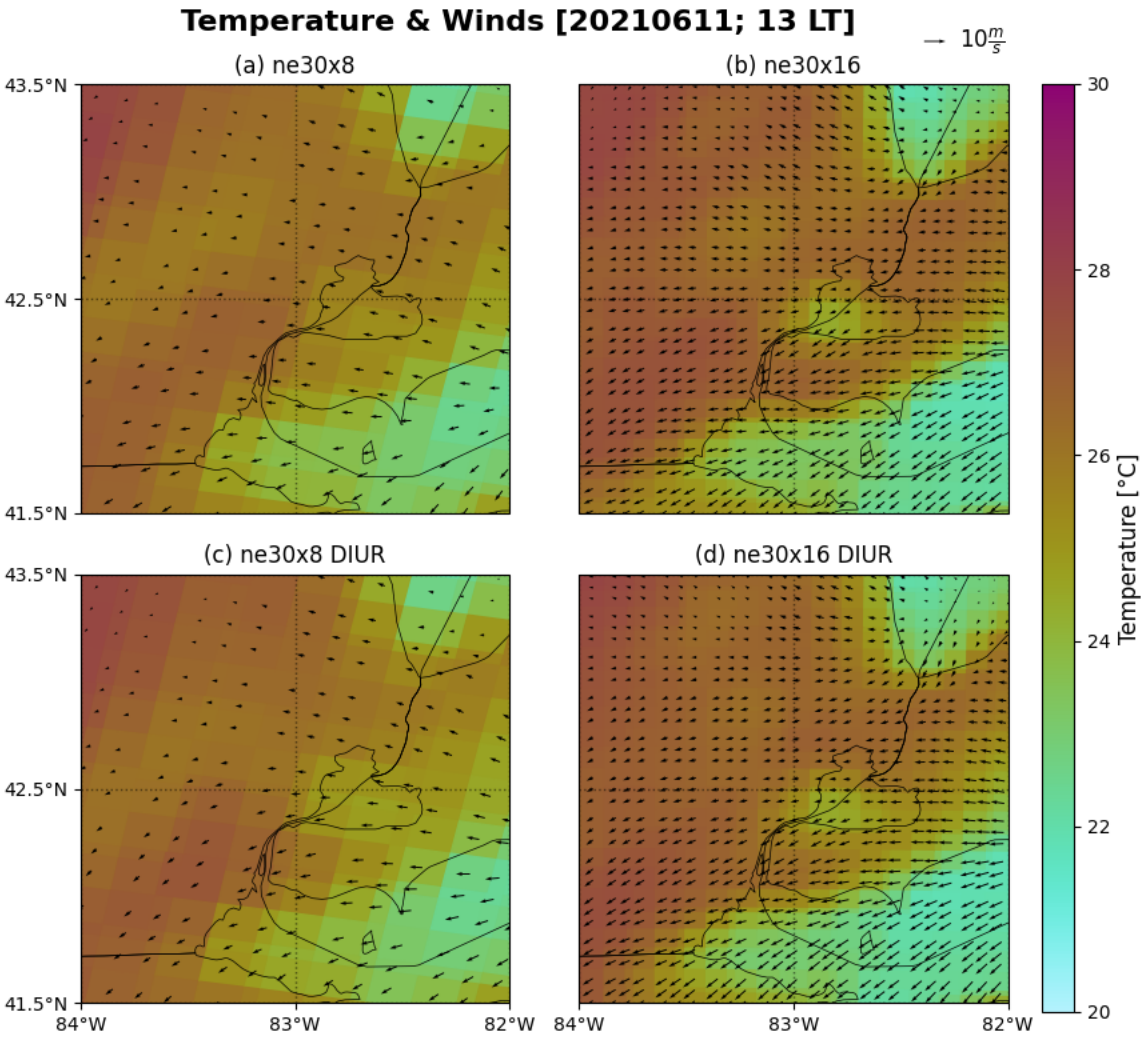

719

720 Figure S20: Modeled temperature and wind vectors for 20210611 at 13 LT.

721

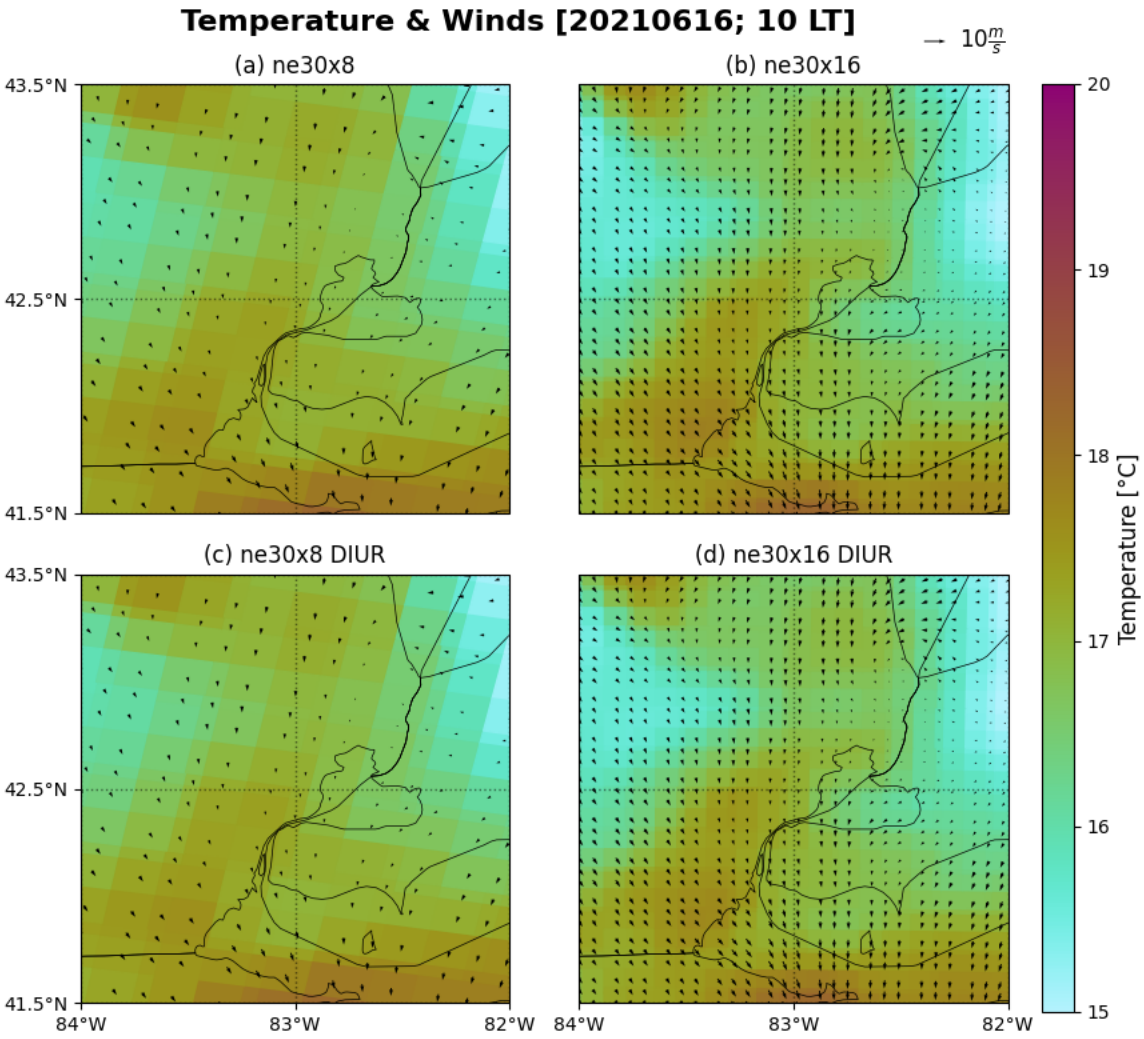

722

723 Figure S21: Modeled temperature and wind vectors for 20210616 at 10 LT.

724

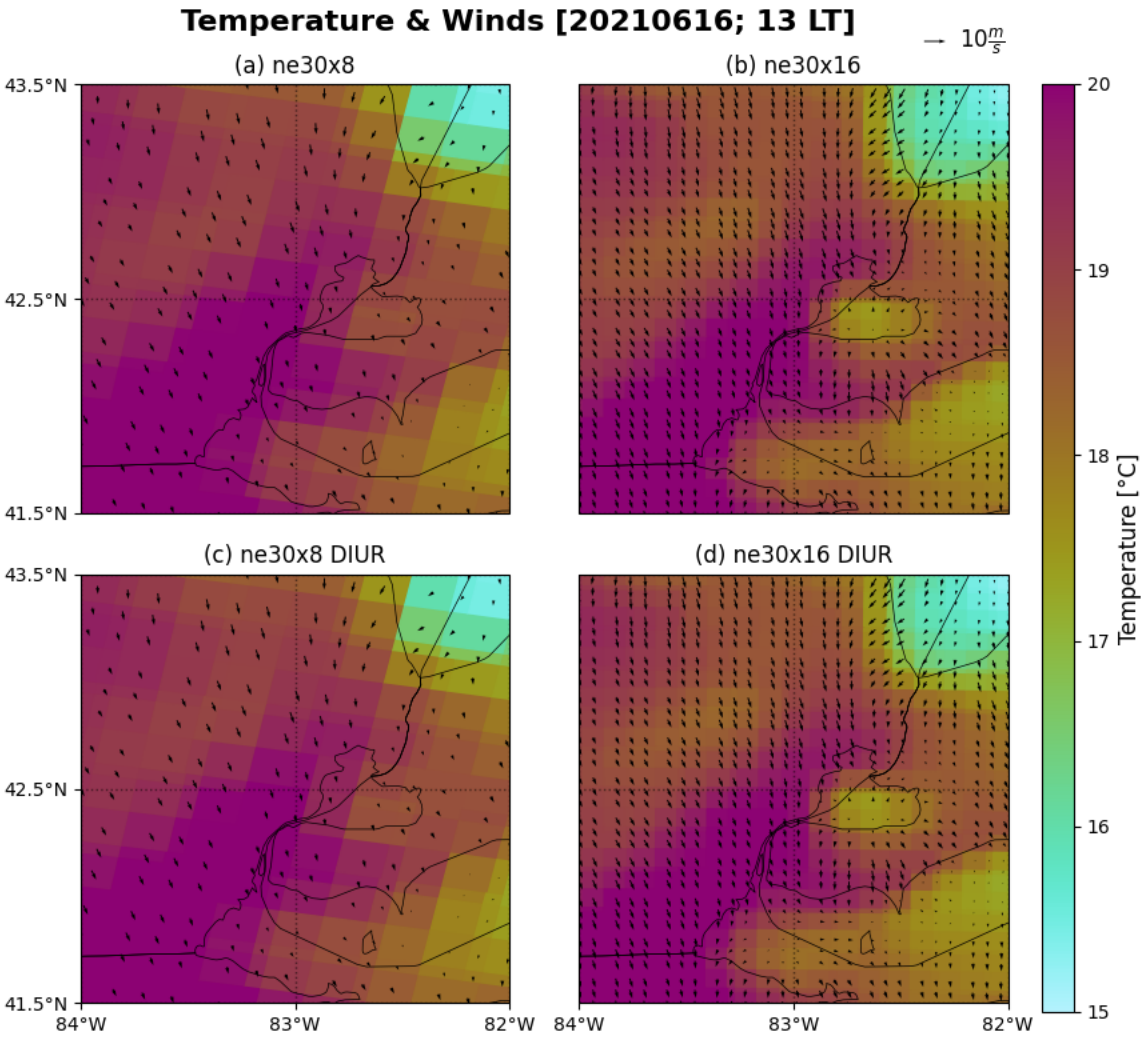

Figure S22: Modeled temperature and wind vectors for 20210616 at 13 LT.

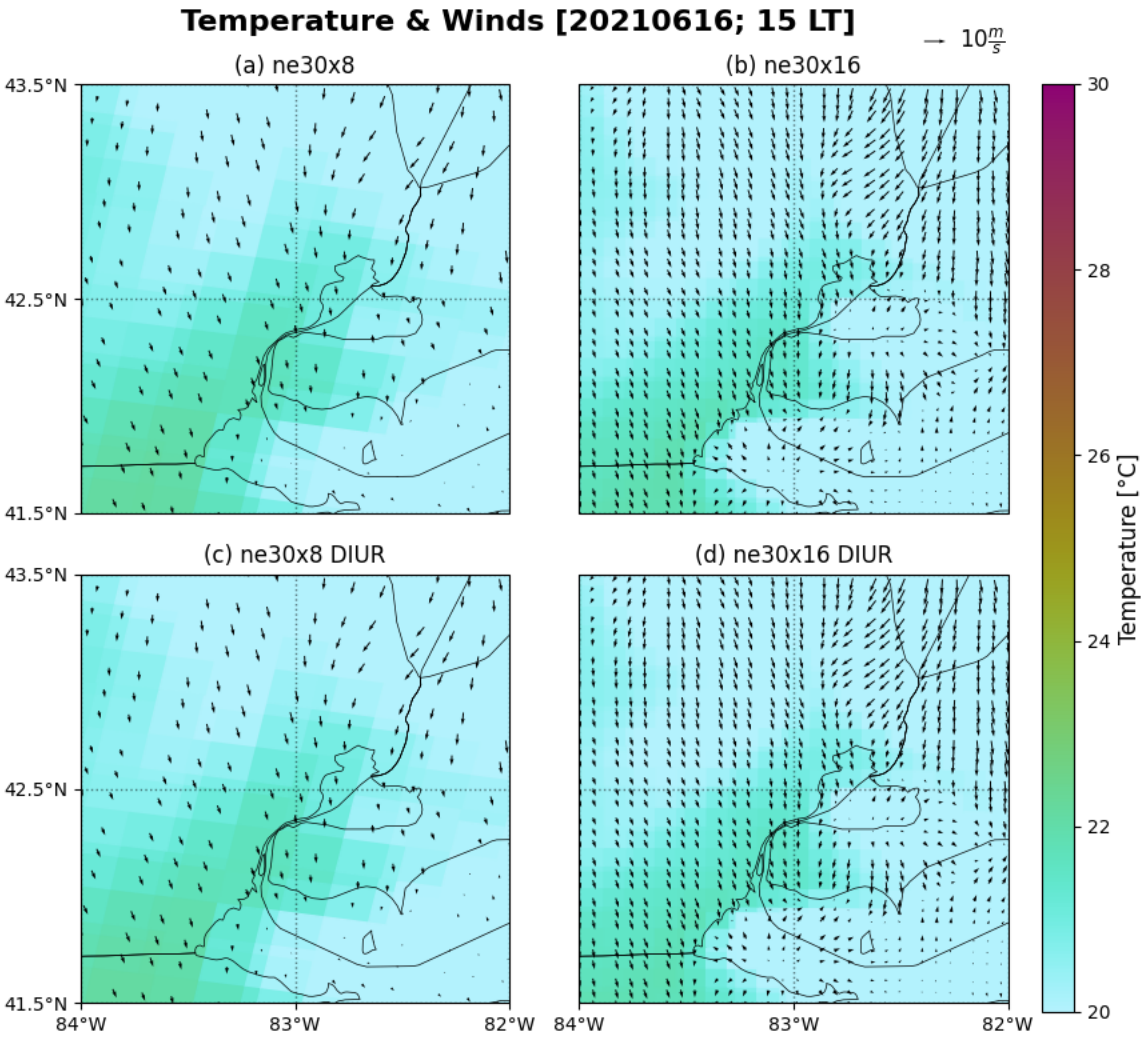

Figure S23: Modeled temperature and wind vectors for 20210616 at 15 LT.

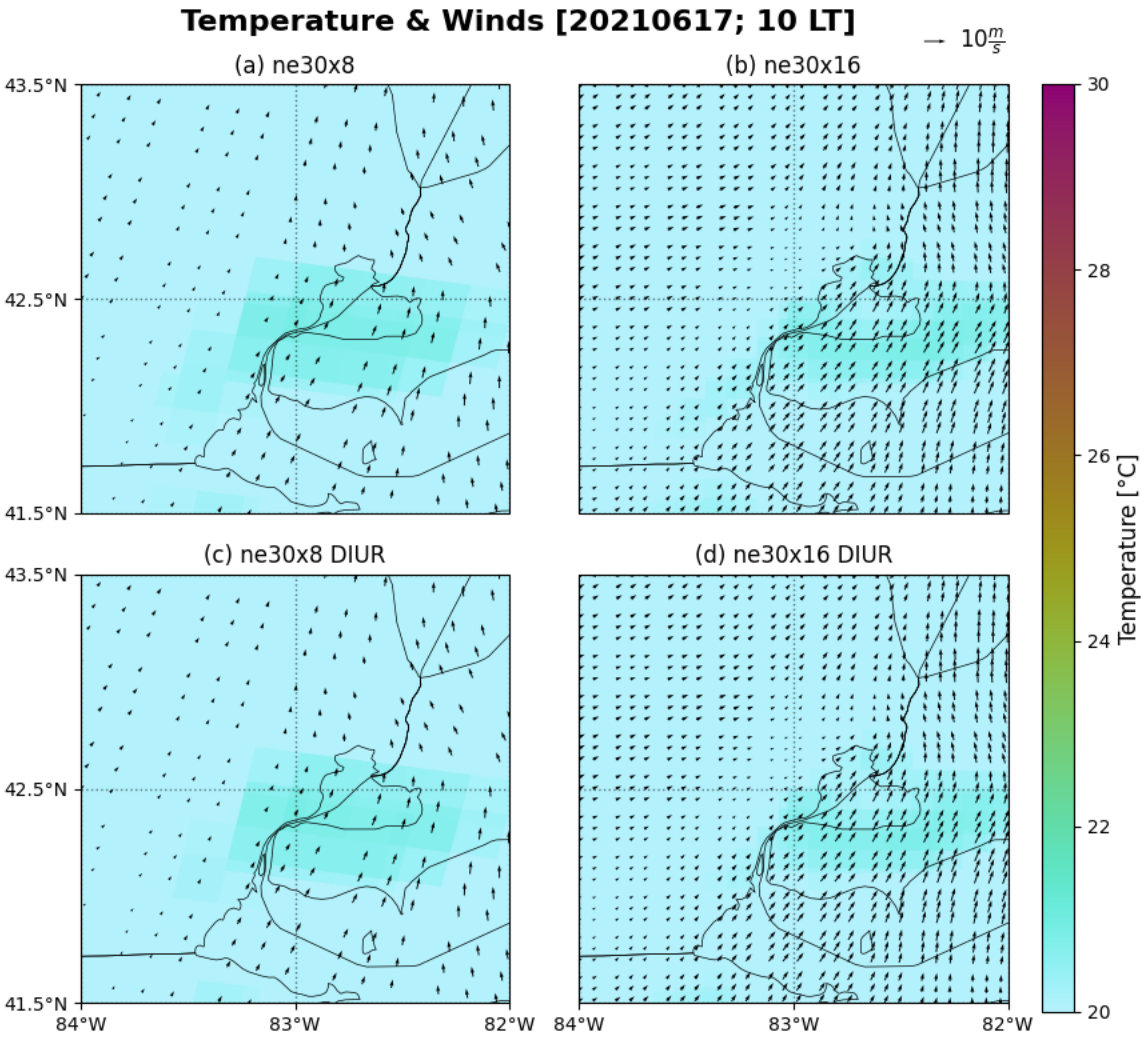

731

732 Figure S24: Modeled temperature and wind vectors for 20210617 at 10 LT.

733

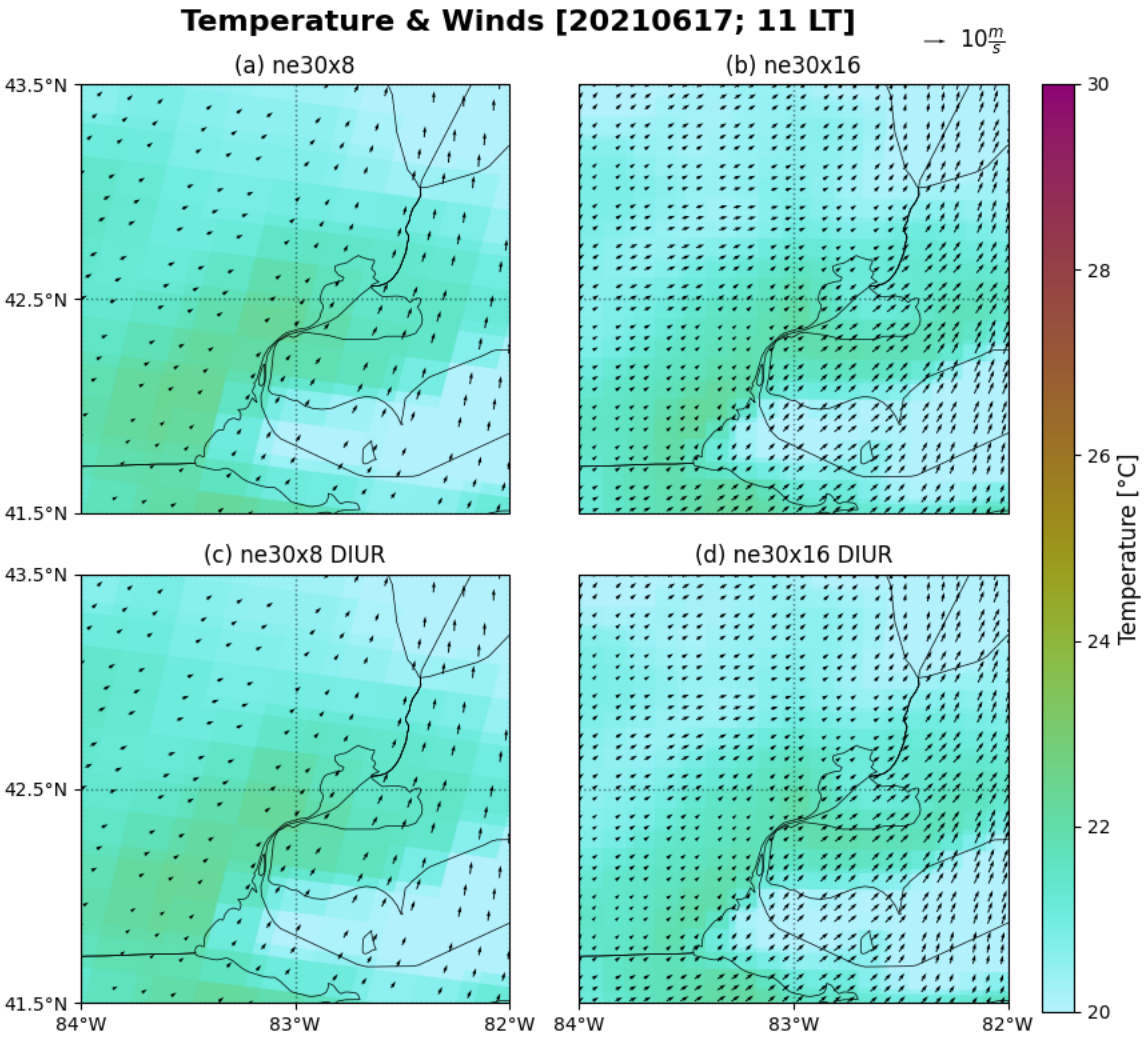

734

735 Figure S25: Modeled temperature and wind vectors for 20210617 at 11 LT.

736

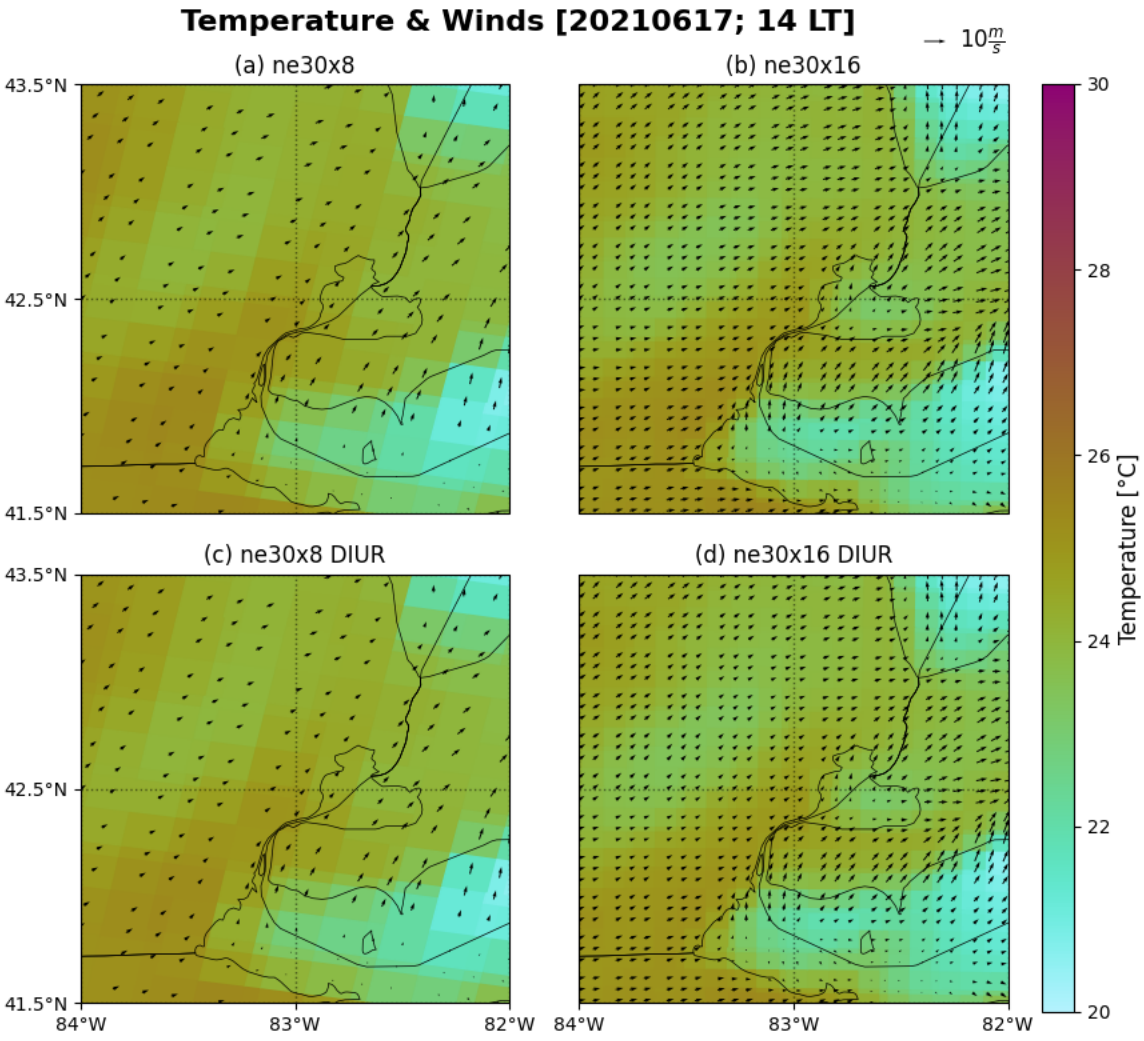

737

738 Figure S26: Modeled temperature and wind vectors for 20210617 at 14 LT.

739

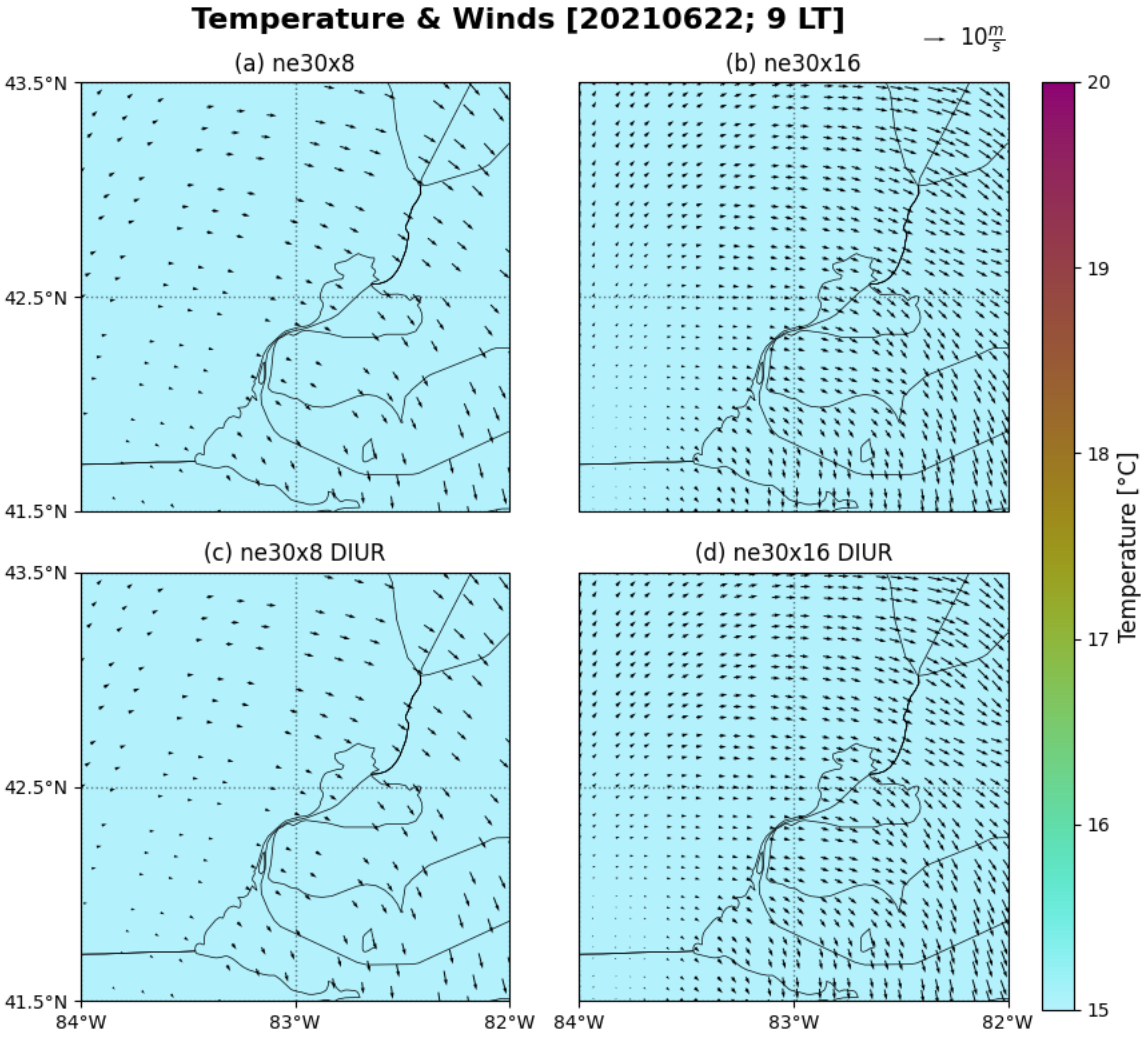

Figure S27: Modeled temperature and wind vectors for 20210622 at 9 LT.

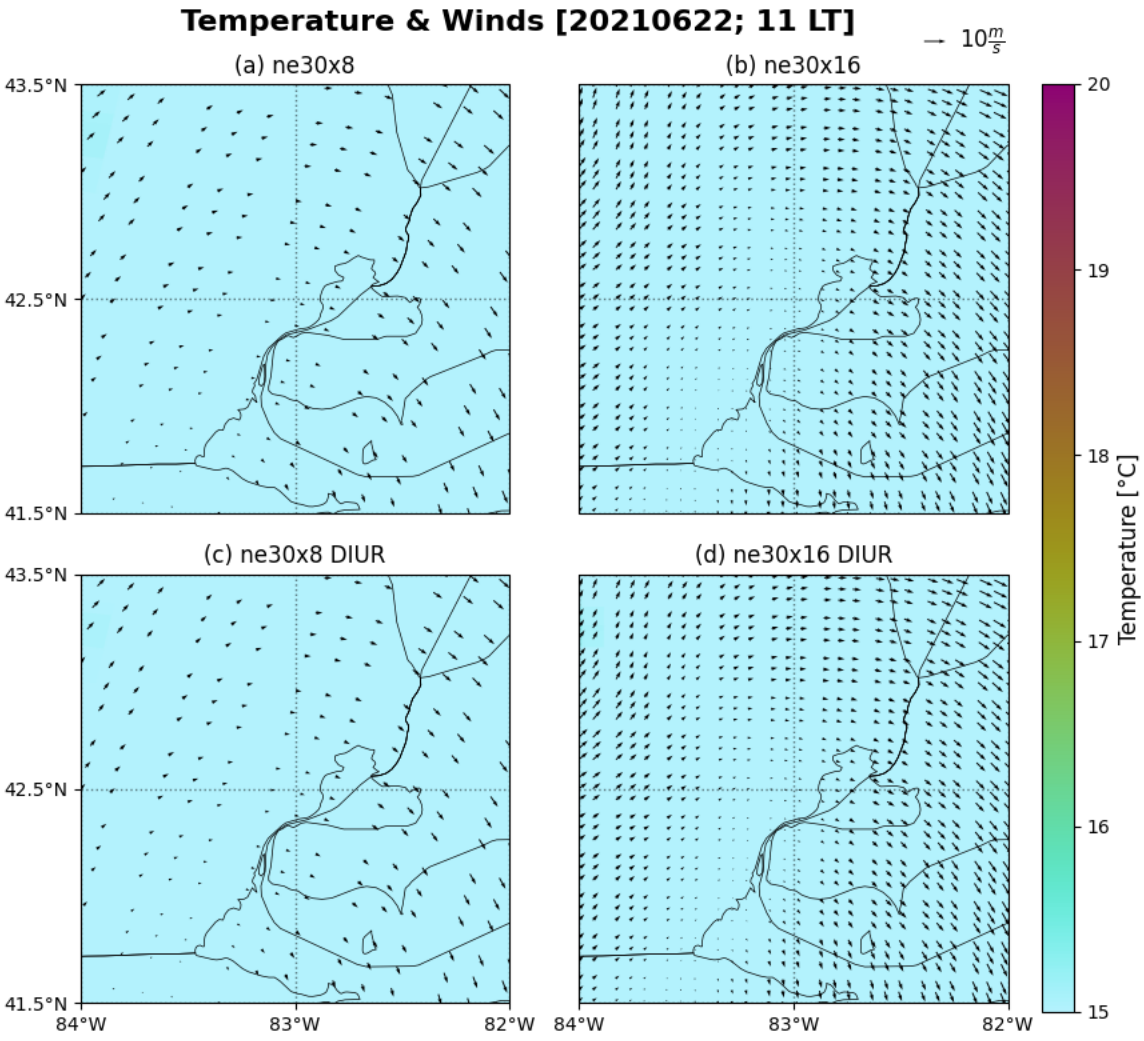

743

744 Figure S28: Modeled temperature and wind vectors for 20210622 at 11 LT.

745

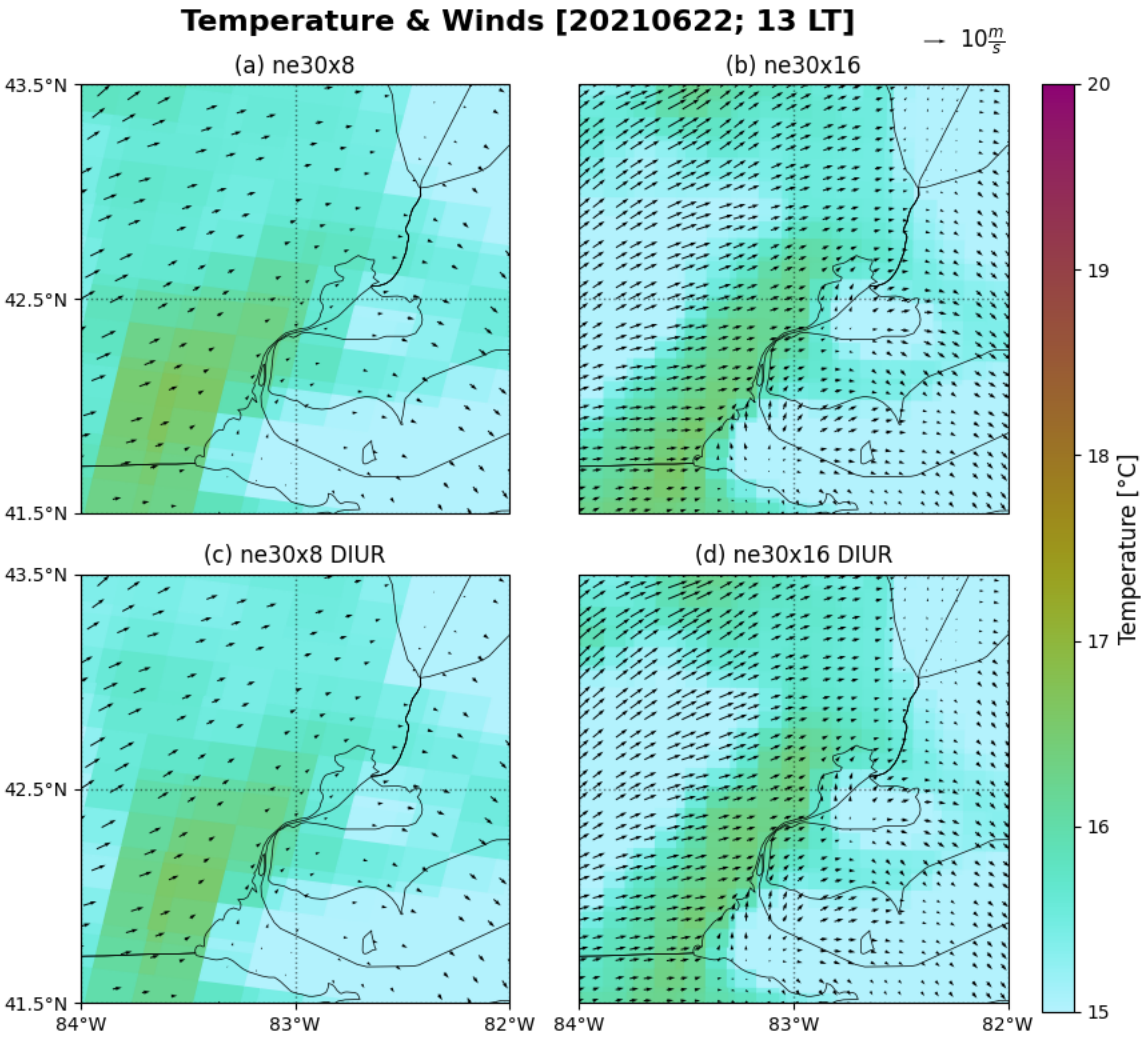

Figure S29: Modeled temperature and wind vectors for 20210622 at 13 LT.

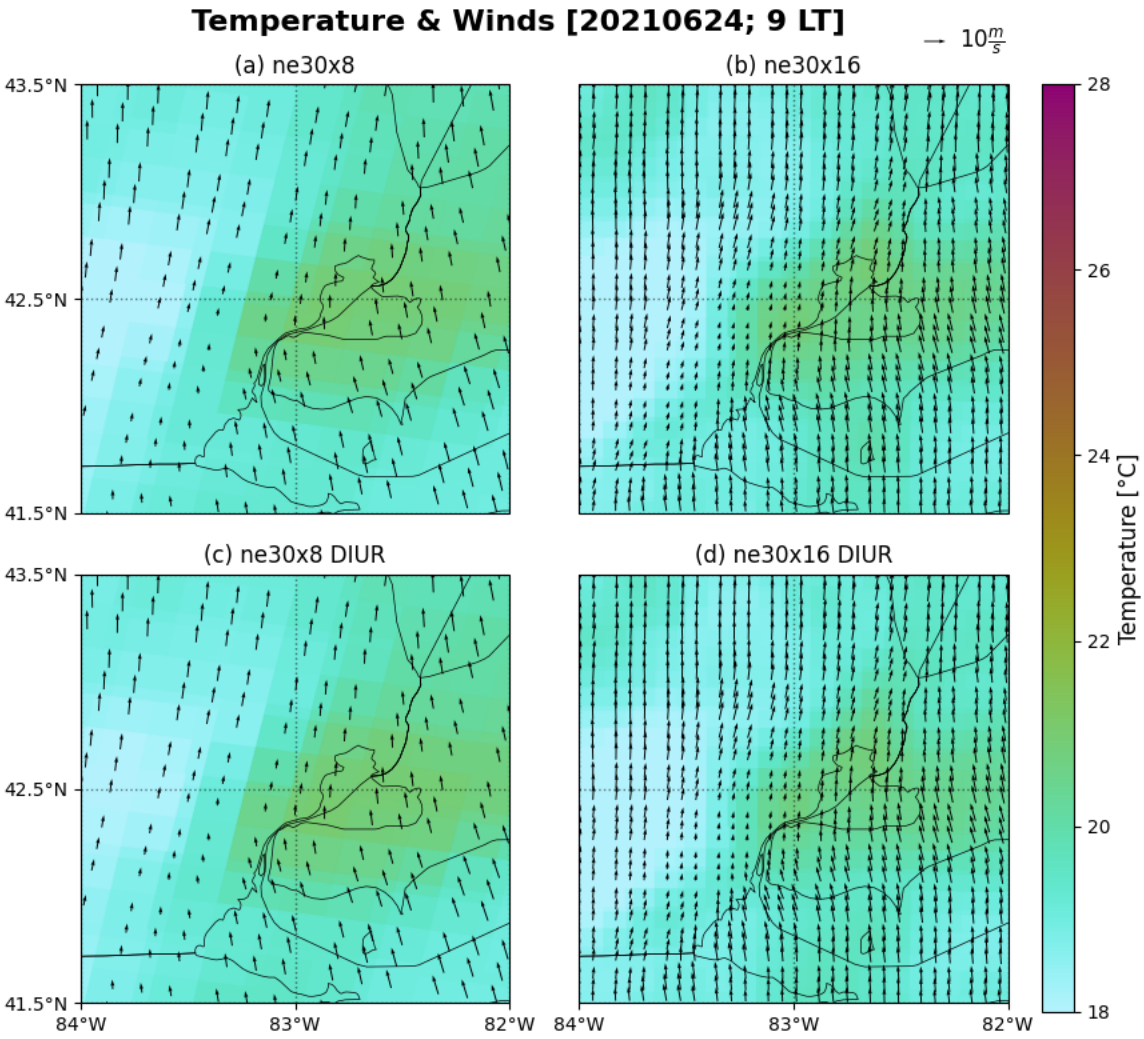

748

749 Figure S30: Modeled temperature and wind vectors for 20210624 at 9 LT.

750

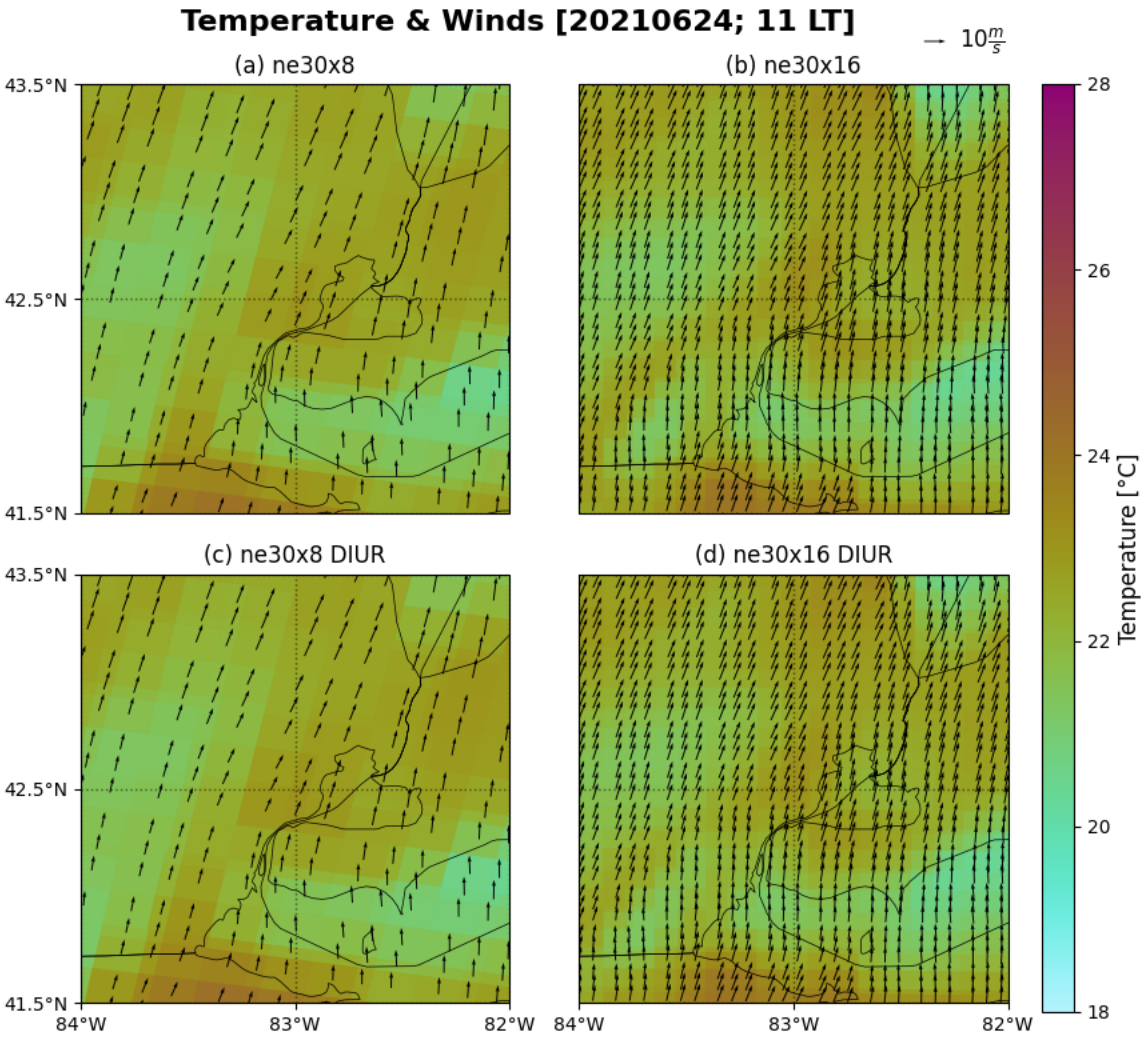

Figure S31: Modeled temperature and wind vectors for 20210624 at 11 LT.

762 **References**

763 Darmenov, A. S. and da Silva, A. M.: The Quick Fire Emissions Dataset (QFED): Documentation of Versions 2.1, 2.2 and
764 2.4: Technical Report Series on Global Modeling and Data Assimilation - Volume 38, 2015.
765
766
767